

RESEARCH

Open Access



# Unravelling the tectonic evolution of the Dinarides—Alps—Pannonian Basin transition zone: insights from structural analysis and low-temperature thermochronology from Ivanščica Mt., NW Croatia

Matija Vukovski<sup>1\*</sup>, Marko Špelić<sup>1</sup>, Duje Kukoč<sup>1</sup>, Tamara Troskot-Čorbić<sup>2</sup>, Tonći Grgasović<sup>1</sup>, Damir Slovenec<sup>1</sup> and Bruno Tomljenović<sup>3</sup>

## Abstract

A comprehensive study, including geological mapping, structural and thermochronological analysis, has been carried out on Ivanščica Mountain (NW Croatia), with the aim to reconstruct the tectonic history of the Dinarides, Southern/Eastern Alps and Pannonian Basin transitional zone. Implementation of structural and thermochronological methods enabled a subdivision of Ivanščica Mt. into two structural domains (from bottom to top): Ivanščica Parautochthon and Ivanščica Imbricate Fan and Cenozoic sedimentary cover. In addition, a sequence of deformational events in tectonic history of this transitional zone is proposed, comprising three extensional and four contractional events starting from Middle Triassic until present times. The two oldest deformational events indicate Middle Triassic (D1) and Early Jurassic (D2) extensional pulses and only occur in volcano-sedimentary successions of the Ivanščica Mt. The oldest contractional event (D3) is related to the obduction of a Neotethyan ophiolitic mélangé over an Upper Triassic to Lower Cretaceous succession of the eastern margin of the Adriatic microplate, which resulted in thermal overprint of the Ivanščica Imbricate Fan structural domain in Berriasian—Valanginian times (~ 140 Ma). This event was soon followed by a second contractional event (D4), which resulted in thrusting and imbrication of the Adriatic passive margin successions together with previously emplaced ophiolitic mélangé, thermal overprint of the footwall successions, fast exhumation and erosion. Apatite fission track data together with syn-tectonic deposits indicate an Hauterivian to Albian age of this D4 event (~ 133–100 Ma). These Mesozoic structures were dextrally rotated in post-Oligocene times and brought from the initially typically Dinaridic SE striking and SW verging structures to the recent SW striking and NW verging structures. The following extensional event (D5) is associated with the formation of SE striking and mostly NE dipping normal listric faults, and ENE striking dextral faults accommodating top-NE extension in the Pannonian Basin. Deformations were coupled with hanging wall sedimentation of Ottnangian to middle Badenian (middle Burdigalian to upper Langhian; ~ 18–14 Ma) syn-rift deposit as observed from the reflection seismic and well data. A short-lasting contraction (D6) was registered in the late Sarmatian (late Serravallian; ~ 12 Ma). The youngest documented deformational event (D7) resulted in reactivation of ENE striking dextral faults, formation of SE

Handling editor: Stefan Schmid

\*Correspondence:

Matija Vukovski  
mvukovski@hgi-cgs.hr

Full list of author information is available at the end of the article



© The Author(s) 2024. **Open Access** This article is licensed under a Creative Commons Attribution 4.0 International License, which permits use, sharing, adaptation, distribution and reproduction in any medium or format, as long as you give appropriate credit to the original author(s) and the source, provide a link to the Creative Commons licence, and indicate if changes were made. The images or other third party material in this article are included in the article's Creative Commons licence, unless indicated otherwise in a credit line to the material. If material is not included in the article's Creative Commons licence and your intended use is not permitted by statutory regulation or exceeds the permitted use, you will need to obtain permission directly from the copyright holder. To view a copy of this licence, visit <http://creativecommons.org/licenses/by/4.0/>.

striking dextral faults as well as the formation of E to ENE trending folds and reverse faults. This event corresponds to late Pannonian (late Messinian; ~6 Ma) to Present NNW-SSE contraction driven by the indentation and counterclockwise rotation of Adriatic microplate. Recognized tectonic events and their timings indicate that Ivanščica was mainly affected by deformational phases related to the Mesozoic evolution of the Neotethys Ocean as well as Cenozoic opening and inversion of the Pannonian Basin. Therefore, the Mesozoic tectono-sedimentary evolution of Ivanščica Mountain proves the paleogeographic affiliation of its non-ophiolitic Mesozoic structural-stratigraphic entities to the Pre-Karst unit of the Dinarides.

**Keywords** Northern Neotethys, Adriatic passive margin, Ophiolite obduction, Nappe stacking, Imbricate fan, Structural inheritance, Tectonic inversion, Pre-Karst unit

## 1 Introduction

Synchronous mountain building of neighbouring orogens often results in complex structural architectures and overprinting relationships. Such complex relationships can only be resolved by comprehensive studies that integrate lithostratigraphic, structural and thermochronological data obtained at local to regional scales of observations. In particular, such an approach is required in cases when both orogens are affected by post-orogenic extensional and/or strike-slip tectonics, a geodynamic scenario known from the past and at present in almost all peri-Mediterranean orogens (e.g., Meulenkamp et al., 1988; Jolivet & Faccenna, 2000; Faccenna et al., 2004, 2013; Kissling et al., 2006). This scenario, which commonly includes post-orogenic local- to regional-scale translations and rotations of differently sized tectonic blocks dismembered from previously formed collisional nappe stacks, is also known from the Dinarides—Alps—Pannonian Basin transitional zone (Fig. 1; e.g., Placer, 1999a; Haas et al., 2000; Tomljenović et al., 2008; van Gelder et al., 2015). This area records complex tectonic histories in the orogenic build-up of the Southern and Eastern Alps as well as the Dinarides, followed by several phases of extension and contraction in the tectonic evolution of the SW margin of the Pannonian Basin (e.g., Fodor et al., 1998; Vrabec & Fodor, 2006; Tomljenović & Csontos, 2001; van Gelder et al., 2015; Fodor et al., 2021). Here, Mesozoic formations of both Alps and Dinarides preserve records of geodynamic processes that resulted with opening and closure of the northern branch of the Neotethys Ocean (e.g., Pamić et al., 1998; Pamić, 2002;

Schmid et al., 2008; 2020; Ustaszewski et al., 2010; the Balkan Neotethys sensu van Hinsbergen et al., 2020). In addition, the Alps record a separate and younger collisional event related to the closure of the Alpine Tethys Ocean (e.g., Neubauer et al., 1999; Willingshofer et al., 1999a; Schmid et al., 2008; 2020; van Hinsbergen et al., 2020). Both oceanic realms contemporaneously existed during a part of Mesozoic times, separating the Adria microplate from Eurasia (e.g., van Hinsbergen et al., 2020). However, during the time of their closure, which differs for each of these oceanic realms, the Adriatic microplate was in a different tectonic position with respect to the European plate: lower plate in the Dinarides and upper plate in the Alps (e.g., Doglioni et al., 1999; Schmid et al., 2008, 2020).

Due to the complex Mesozoic and Cenozoic geodynamics at the Dinarides-Southern/Eastern Alps-Pannonian Basin transitional zone (Fig. 1a, b), a detailed reconstruction of the tectonic and depositional history, in its part in the northern Croatia, is still lacking. Among several inselbergs in this area (Fig. 1c), Medvednica Mt. is the most comprehensively studied so far, providing a large data set on different topics regarding Mesozoic stratigraphy (e.g., Halamić et al., 1999, 2005; Babić et al., 2002, with references therein), metamorphic and igneous petrology (e.g., Belak & Tibljaš, 1998; Slovenec & Pamić, 2002; Lugović et al., 2007; Judik et al., 2008; Belak et al., 2022; Mišur et al., 2023;), paleomagnetism, structural architecture and tectonics (e.g., Tomljenović et al., 2008; van Gelder et al., 2015). The results of most of these studies, in

(See figure on next page.)

**Fig. 1** **a** Topographic map of the northern Adriatic realm. Note the red polygon representing outlines of Ivanščica Mt. **b** Tectonic map after Schmid et al. (2020) showing constituent tectonic units of the Dinarides and the Alps. Ivanščica Mt. (marked with yellow line) occupies position at the junction of the Western Vardar ophiolitic unit of the Dinarides and South Alpine unit of the Alps in the southwestern part of the Pannonian Basin (white outlines). PFS—Periadriatic Fault System. Location of figure is shown in **a**. **c** Geological map of the Ivanščica Mt. and wider surrounding area in the Dinarides—Alps—Pannonian Basin transitional zone (simplified and modified after Basic Geological Maps of former Yugoslavia on the 1:100,000 scale, sheets Celje (Buser, 1977), Rogatec (Aničić & Juriša, 1984), Varaždin (Šimunić et al., 1982), Novo Mesto (Pleničar et al., 1975), Zagreb (Šikić et al., 1977) and Ivanić (Basch, 1981)). Location of figure is shown in **b**

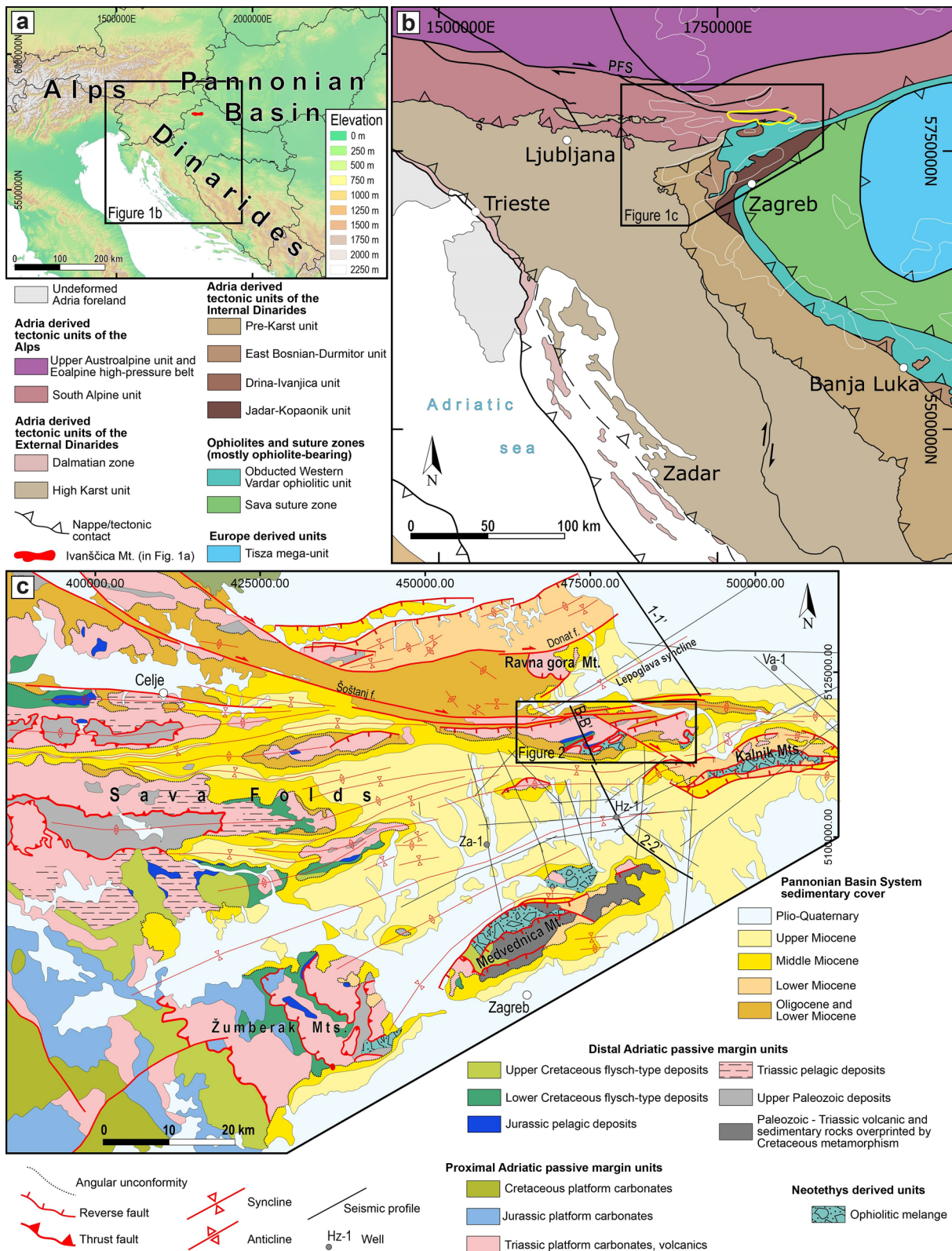


Fig. 1 (See legend on previous page.)

combination with data from the Basic Geological Map of Yugoslavia, sheet Rogatec (Aničić & Juriša, 1984) and sheet Varaždin (Šimunić et al., 1982), were so far used for the correlation of pre-Neogene tectonic units in this transitional zone, only exposed in inselbergs, with corresponding tectonic units defined within a much wider surrounding area (e.g., Haas et al., 2000; van Gelder et al., 2015) and across the entire Alpine-Carpathian-Dinaridic-Hellenic orogenic system (e.g., Schmid et al., 2008, 2020; van Hinsbergen et al., 2020). Compared with the neighbouring Medvednica Mt., modern data on the geology of the Ivanščica Mt. were relatively scarce (Babić et al., 2002; Goričan et al., 2005; Lužar-Oberiter et al., 2009, 2012), until recently when a series of studies were released by the 'GOST' project (<https://projectgost.wordpress.com>). These studies provide new data set on stratigraphy (Slovenec et al., 2020; Kukoč et al., 2023, 2024), petrology (Slovenec & Šegvić, 2024; Slovenec et al., 2023; Šegvić et al., 2023) and lithostratigraphy of the Adriatic passive margin successions (Vukovski et al., 2023), tectonically assembled into the structural architecture of Ivanščica Mt.

Being a supplement to published studies of the GOST project, this paper aims to present new and more detailed data on the spatial arrangement, kinematics and age of deformational structures in Mesozoic and Cenozoic rocks of Ivanščica Mt. and neighbouring area. These data were obtained by a multi-scale structural analysis, including geological mapping, interpretation of reflection seismic sections, vitrinite reflectance and apatite fission track measurements. After a short overview on geological and structural setting of Ivanščica Mt. based on previously published data, this paper presents new data on the structural architecture and low-temperature thermochronology of the study area.

These data are then used to propose a sequence of deformational events in the study area. The presented deformational sequence is correlated with deformational events revealed in neighbouring areas of the Dinarides, Southern and Eastern Alps and SW Pannonian Basin. Obtained deformational events are discussed in the context of tectonic evolution of the region, starting from the Middle Triassic until present. Finally, we propose a new correlation between the established tectonic units of Ivanščica Mt. with those known from the Internal Dinarides.

## 2 Geological setting of Ivanščica Mountain

Ivanščica Mt. is built by upper Paleozoic and Mesozoic sedimentary successions belonging to the northern Gondwana margin and later to the Adriatic margin, a Neotethyan ophiolitic mélangé and an uppermost

Oligocene to Quaternary sedimentary cover (Figs. 2, 3; Šimunić et al., 1982; Aničić & Juriša, 1984).

### 2.1 Lithostratigraphic characteristics of Paleozoic and Mesozoic rock units

The oldest rocks on Ivanščica Mt. are Permian brown-red conglomerates, sandstones and black shales conformably overlain by Lower Triassic clastic deposits, including sporadic 1–2 m thick dolomite layer along the contact (Šimunić et al., 1982; Šimunić & Šimunić, 1997). Lower Triassic sediments consist of micaceous sandstone, mica siltstone, shale and marl in the lower part and dark-grey, tabular, thin-bedded limestone in the upper part (Šimunić & Šimunić, 1997). Paleozoic and Lower Triassic deposits have spatially limited exposure on the northern slopes of the mountain. These deposits originated from a shallow-marine environment (Šimunić et al., 1982).

The largest part of the mountain is built up of several hundred meters thick Middle Triassic deposits, predominantly shallow-marine dolomite and limestone (Fig. 2; Šimunić et al., 1982). Pelagic successions consisting of upper Anisian to Ladinian pelagic limestone and radiolarian chert are intercalated with basic to acidic volcanic and volcanoclastic lithologies (Goričan et al., 2005; Slovenec et al., 2020, 2023; Kukoč et al., 2023; Smirčić et al., 2024). These pelagic successions are several tens of meters thick, tectonically deformed and their contacts with the underlying and overlying formations are rarely exposed. Deep-marine basins formed during this period were relatively short-lived and carbonate platform sedimentation was reestablished in the Late Ladinian (Goričan et al., 2005). Upper Triassic sediments of Ivanščica Mt. are exclusively shallow-marine and consist of several hundred meters thick series of dolomite and limestone (Šimunić et al., 1982; Šimunić & Šimunić, 1997). These are the equivalent of the Hauptdolomit and Dachstein Limestone found in the Alps (Vukovski et al., 2023). Lower Jurassic to Lower Cretaceous deposits are exposed in the central part of Ivanščica Mt. The successions composed of these deposits differ in the southern and northern parts of central Ivanščica Mt. (Fig. 2). In the northern part, shallow-marine Lower Jurassic limestone conformably overlies Upper Triassic carbonates and is in turn overlain by Middle Jurassic pelagic limestone (Fig. 3; Vukovski et al., 2023). In contrast, in the southern part, Upper Triassic deposits are overlain by Lower Jurassic thick pelagic series consisting of pelagic limestone, carbonate breccia, marl and calcarenite (Fig. 3; Babić, 1974; Vukovski et al., 2023). Middle to Upper Jurassic radiolarian cherts are recorded in both areas, however, their contact with underlying deposits and complete thickness is not known. In both areas, radiolarian cherts conformably pass up-section into Tithonian to Valanginian



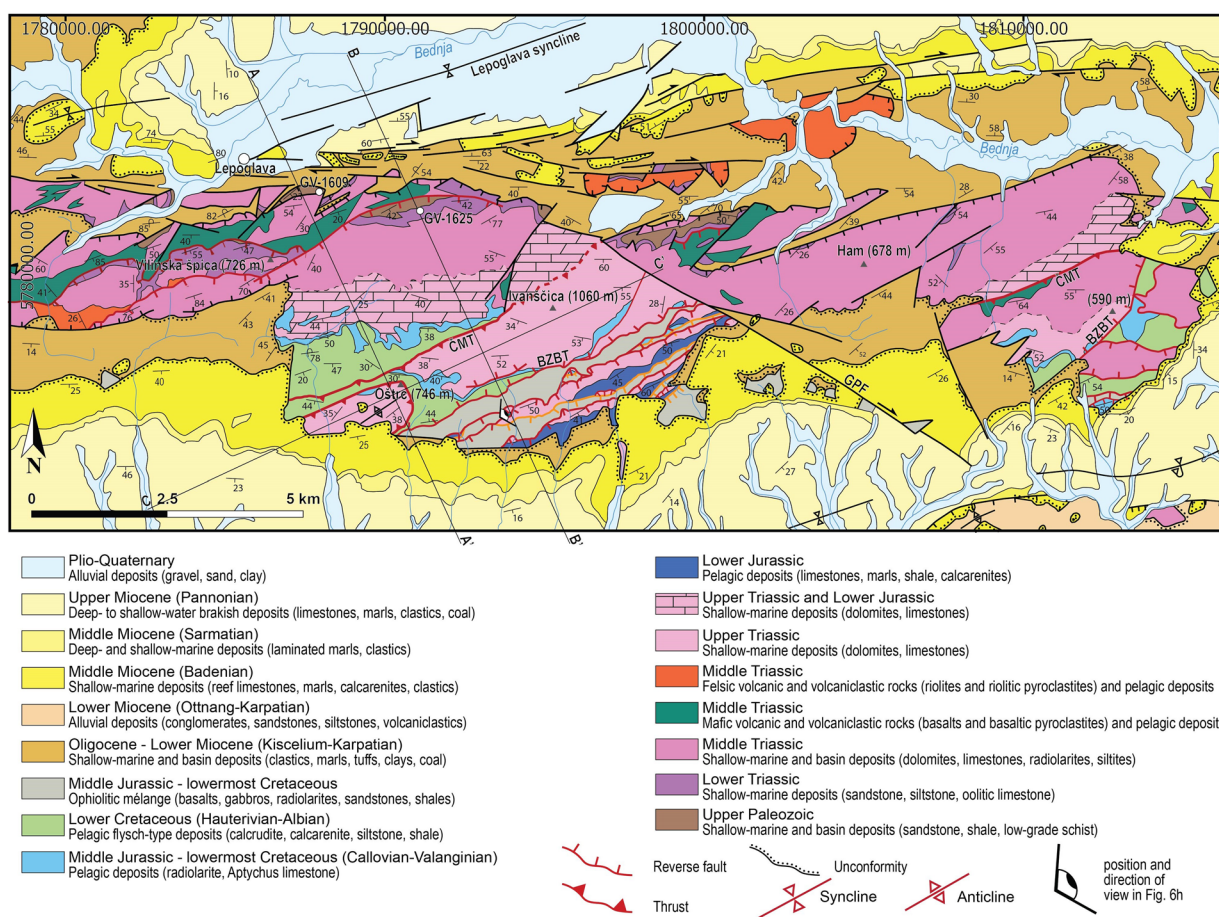


**Fig. 2** Geological map of Ivanščica Mt. compiled from Šimunić et al. (1982) and the results of this study. The map shows the locations of cross-sections **A-A'**; **B-B'** and **C-C'** (shown in Fig. 5) and sample locations used for apatite fission track dating. The location of the figure is shown in Fig. 1c. For colour coding of the tectonic features, please refer to Fig. 3. *ČMT* Črne Mlake thrust, *BZBT* Babin Zub back-thrust, *GPF* Gotalovec-Prigorec fault

pelagic Aptychus limestone with several beds of calcarenites sporadically occurring at the contact as recorded in the southern part of central Ivanščica (Fig. 3; Babić & Zupanić, 1973; Vukovski et al., 2023). The youngest Mesozoic deposits are mixed carbonate-siliciclastic turbidites of the Hauterivian to Albian Ostrc Formation (Zupanić et al., 1981; Lužar-Oberiter et al., 2009, 2012), which overly the Aptychus limestone. On the southern slopes of Ivanščica Mt., in its central and eastern parts, an ophiolitic mélangé is widely exposed, named as the Repno complex (Fig. 2; Babić & Zupanić, 1978; Babić et al., 2002). This ophiolitic mélangé is composed of centimeter to hundred meters sized blocks of sandstone, chert, basalt and gabbro chaotically embedded within a shaly-silty matrix (Babić et al., 2002; Slovenec et al., 2011; Kukoč et al., 2024). The age of the blocks varies from late Anisian to late Oxfordian (Slovenec et al., 2011; Kukoč et al., 2024) while the ages derived from palynomorphs

found in the matrix ranges from Hettangian to Bajocian (Babić et al., 2002).

Permian to Middle Triassic deposits were mostly deposited in the shallow-marine depositional environments along the northern Gondwana margin. Middle Triassic successions reflect a period of intense tectonic activity related to the continental rifting and break-up of Gondwana, which resulted in the opening of the Neotethys Ocean and formation of the Adriatic passive margin with horst-and-graben depositional environments (Goričan et al., 2005; Kukoč et al., 2023). Upper Triassic to Lower Cretaceous sedimentary successions of Ivanščica Mt. are interpreted as deposited on the eastern passive margin of the Adria microplate (Lužar-Oberiter et al., 2012; Vukovski et al., 2023), which was facing the evolving Neotethys Ocean from the Middle Triassic until the ophiolite obduction in latest Jurassic-earliest Cretaceous (Schmid et al., 2008, 2020). Sedimentation on the

margin reflected regional tectonic activity. Resedimented shallow-marine material was likely supplied from the adjacent Adriatic Carbonate Platform (Vukovski et al., 2023). Hauterivian to Albian turbidites of the Oštrc Fm. have been interpreted as deposited in a clastic wedge in front of the advancing nappes carrying the Neotethys ophiolites (Lužar-Oberiter et al., 2009, 2012). The ophiolitic mélange is interpreted to have formed during the Middle Jurassic intra-oceanic subduction in the northern branch of the Neotethys Ocean (Western Vardar ophiolitic unit sensu Schmid et al., 2020) and subsequent Late Jurassic to earliest Cretaceous obduction of ophiolites of this oceanic realm on the eastern Adriatic margin (Babić et al., 2002; Kukoč et al., 2024).

## 2.2 Lithostratigraphic characteristics of Cenozoic rock units

The oldest Cenozoic deposits on Ivanščica Mt. comprise upper Egerian (lower Aquitanian) clastic deposits with coal seams (Fig. 3; Šimunić et al., 1982). On the southern slopes of the mountain, these deposits lay unconformably over different Mesozoic formations, locally also in tectonic contact with underlying Mesozoic formations (Fig. 2). On the northern slopes, upper Egerian (lower Aquitanian) clastic deposits are found in tectonic contact and steeply dip underneath the Mesozoic formations (Figs. 2, 5; Šimunić et al., 1982). In the neighboring area, only a few kilometers to the NW, complete Oligocene to Lower Miocene succession of dominantly marine clastic deposits have been described (Aničić & Juriša, 1984; Avanić et al., 2021). This around two kilometers thick Oligocene to Lower Miocene succession is interpreted as deposited within the so-called Hrvatsko Zagorje Basin (Fig. 3), a marginal basin of the Central Paratethys Sea (Avanić et al., 2021). The southern margin of the Hrvatsko Zagorje Basin is interpreted to be located along the present-day southern foothills of Ivanščica Mt. (Pavelić & Kovačić, 2018). Further to the south, the deposition of Cenozoic rocks commenced significantly later, in the Ottnangian (middle to late Burdigalian) or locally even Badenian (Langhian and early Serravallian; Pavelić & Kovačić, 2018). The deposition of Ottnangian to middle Badenian (middle to upper Burdigalian to upper Langhian) alluvial to marine succession with volcanoclastics marks the syn-rift period in the evolution of the newly

formed so-called North Croatian Basin (Fig. 3; Pavelić, 2001; Pavelić & Kovačić, 2018). Further continuation of extension and accompanying transgression resulted in the unification of the Hrvatsko Zagorje and North Croatian basins during the early to middle Badenian (Langhian). Since then, both areas represent a single basin with a uniform lithostratigraphy (Fig. 3), occupying the south-western position in the Pannonian Basin (Pavelić & Kovačić, 2018). Middle Badenian (late Langhian) sediments are predominantly characterised by widespread sedimentation of marls and limestones (Pavelić & Kovačić, 2018). Regional late Badenian (early Serravallian) transgression and cessation of volcanic activity mark the end of the rifting stage and the onset of post-rift thermal subsidence (Pavelić & Kovačić, 2018). Sarmatian (late Serravallian) and early Pannonian (early Tortonian) sediments are characterized by marine to brackish marl and limestone. During the Late Miocene and Pliocene, the brackish lake was continuously in-filled by a turbiditic, deltaic, and finally alluvial clastic sequence (Pavelić & Kovačić, 2018), reflecting the diachronous regressive trend observed across the entire Pannonian Basin (Magyar et al., 2013). These were overlain by Quaternary clastic deposits (Šimunić et al., 1982).

## 2.3 Structural characteristics

Structurally, Ivanščica Mt., together with other mountains in northern Croatia, is considered as the eastern part of an area locally known as the “Sava folds” (Fig. 1c; Šimunić et al., 1979, 1982; Šimunić 1992), a name characterizing a wedge-shaped tectonic domain in the Dinarides—Alps transition zone in eastern Slovenia and northern Croatia, with kilometer-sized E to ENE trending relatively open folds that deformed earlier formed tectonic units during Latest Cenozoic times (Winkler, 1923; Placer, 1999b). During their work on the Basic Geological Map of Yugoslavia, sheet Varaždin, Šimunić et al., (1979, 1982) considered all mapped faults on Ivanščica to be of Cenozoic age, the main contractional deformations occurring during the Miocene. These authors interpreted Ivanščica as a N verging nappe, which brought Paleozoic and Mesozoic formations over upper Oligocene and lowermost Miocene sediments during the Early Miocene (in Eggenburgian; late Aquitanian to early Burdigalian). The occurrences of Triassic-Jurassic carbonates in the

(See figure on next page.)

**Fig. 3** Tectonostratigraphic columns showing detail lithostratigraphy of Middle Triassic to Lower Cretaceous successions of two structural domains and Cenozoic sedimentary cover. Note the difference in the Lower Jurassic deposits of ČMT footwall succession (IP structural domain) and ČMT hanging wall succession (IIF structural domain). Mesozoic lithostratigraphic columns are cut by faults of different ages and ČMT hanging wall succession is doubled in order to schematically show structural setting, ages and relations between different deformational structures as a result of different deformational events. Note the differences and similarities in Cenozoic deposits N of Šoštanj fault and those of Ivanščica Mountain

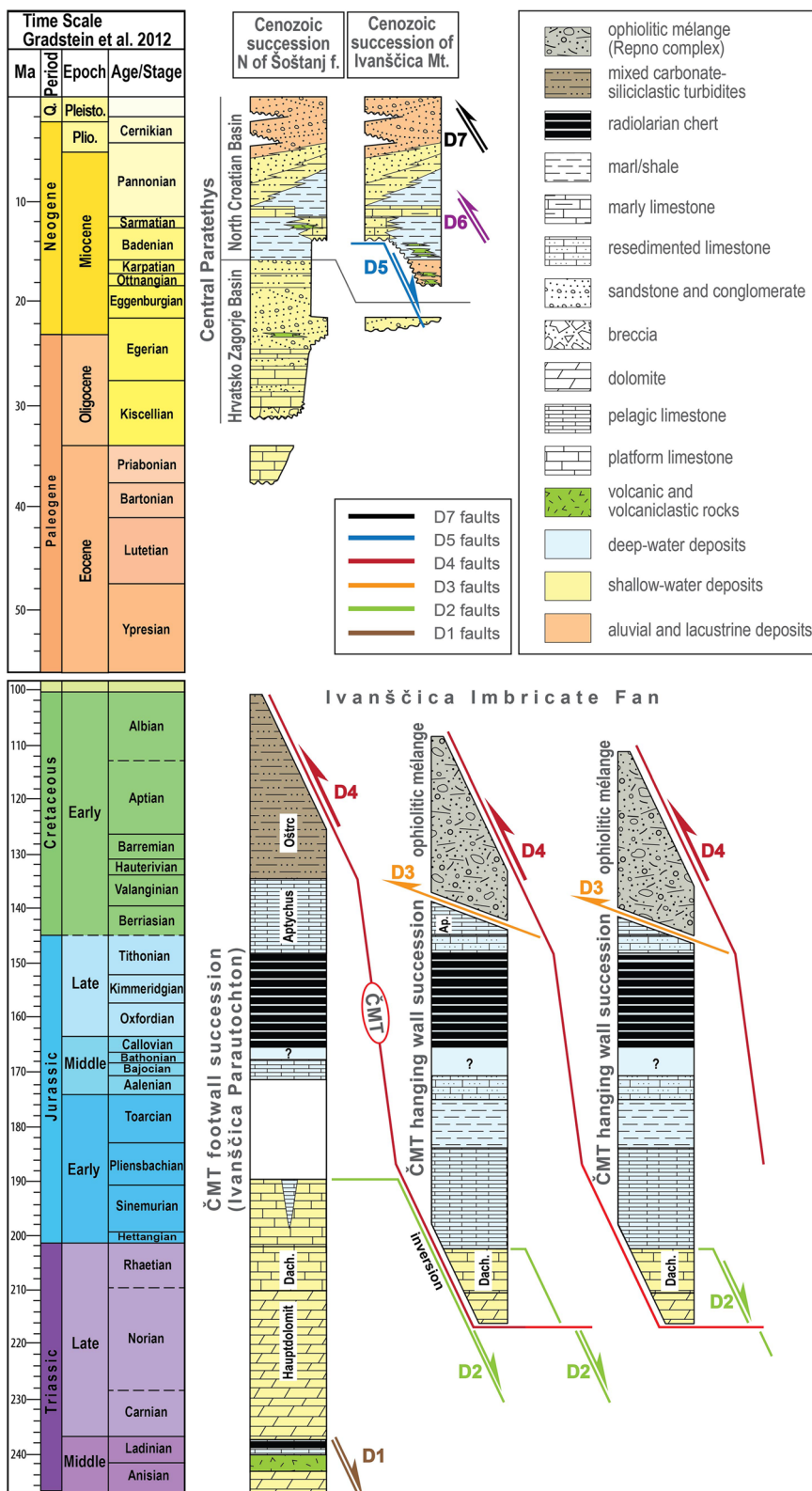


Fig. 3 (See legend on previous page.)



southern part of central Ivanščica were interpreted as erosional remains of a structurally higher nappe (Šimunić et al., 1979, 1982) or as olistoliths embedded in the Repno complex (Babić & Zupanič, 1978). As we will show below, we newly interpret those occurrences as a stack of imbricates built up of Adriatic passive margin successions and the Repno complex that essentially formed during an Early Cretaceous contractional event.

More recent studies consider the northern Croatian mountains, including Ivanščica Mt., to be a part of the Southern Alps unit (Placer, 1999a). According to van Gelder et al. (2015) and Schmid et al. (2008, 2020) the continental units of Ivanščica Mt. are presently a part of the S verging South Alpine nappe emplaced over earlier formed Internal Dinaridic units during Miocene times. Prior to this south directed emplacement, the tectonic block carrying the northern Croatian mountains rotated 130° clockwise in Oligocene–earliest Miocene, as interpreted by Tomljenović et al. (2008). This interpretation is based on paleomagnetic data measured in Upper Cretaceous deposits on Medvednica Mt. The rotation resulted from earliest Miocene eastward lateral extrusion of the Alps and Dinaridic fragments, accompanied by strong dextral displacements along the Periadriatic fault system and Mid-Hungarian fault zone representing its eastern continuation (Fodor et al., 1998; Schmid et al., 2008). A prominent dextral strike-slip Šoštanj fault which tangent northern foothills of Ivanščica Mt. (Fig. 1c) represents the southernmost branch of the Periadriatic fault system (Fig. 1b; Vrabcic & Foor, 2006; Atanackov et al., 2021). Subsequent normal faulting related to Early Miocene rifting and opening of this part of the Pannonian Basin overprinted older structures (Tomljenović & Csontos, 2001; van Gelder et al., 2015). Basin inversion, which was initiated in Late Miocene–Pliocene, caused folding and reverse faulting resulting in the final uplift of the north Croatian mountains (Tomljenović & Csontos, 2001). This inversion was synchronous with approximately 35° counterclockwise (CCW) rotation, active in Late Miocene to recent times, presumably driven by the CCW rotation and indentation of the Adriatic microplate (Tomljenović & Csontos, 2001; Márton et al., 2002).

### 3 Methods and results

#### 3.1 Description of deformational structures

Ivanščica is a densely forested mountain with rather scarce high-quality geological outcrops. For this reason, extensive fieldwork was carried out. At locations considered as essential for better understanding of the deformational history of study area, detailed geological mapping at scales of 1:25,000 and 1:5000 was conducted. Special attention was given to the collection of structural and kinematic data, like orientation of bedding, meso-scale

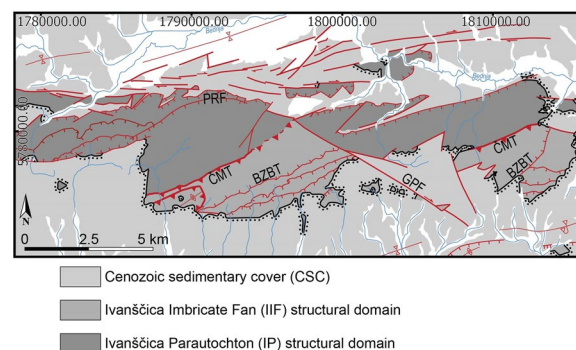


**Fig. 4** Simplified tectonic map of the Ivanščica Mt. showing spatial distribution of structural domains and Cenozoic sedimentary cover. ČMT Črne Mlake thrust, BZBT Babin Zub back-thrust, GPF Gotalovec-Prigorec fault, PRF Prigorec reverse fault

folds, axial planar cleavage, S-C fabrics, intersection lineations, fault planes and their kinematic indicators, many of these recorded for the first time in the area. Based on measured structural data, observed differences in deformation styles and mapped tectonic and depositional contacts shown in maps (Figs. 2, 4) and cross-sections (Fig. 5), the study area is subdivided into two structural domains that are from bottom to top: (1) Ivanščica Parautochthon (IP) and (2) Ivanščica Imbricate Fan (IIF). These are overlain by Cenozoic sedimentary cover (CSC) representing the post-tectonic sedimentary cover regarding the Mesozoic deformational events.

#### 3.1.1 Ivanščica Parautochthon (IP) structural domain

The Ivanščica Parautochthon (IP) structural domain comprises Permo-Mesozoic formations exposed along its northern slopes (Figs. 2, 5). As shown below, our new data do not suggest that IP structural domain would be of allochthonous nature nor do represent a part of a nappe. Therefore, we conclude that parautochthon is an appropriate term for this structurally lower domain. This domain is cut and broken apart into two structural blocks to the west and east of a prominent SE striking Gotalovec–Prigorec dextral strike-slip fault (GPF; see Fig. 2). In both structural blocks, IP structural domain is overthrust by the Ivanščica Imbricate Fan (IIF) structural domain along the SE dipping Črne Mlake roof thrust (ČMT; Figs. 2, 4 and 5). On its SW margin, the IP structural domain is unconformably overlain by upper Egerian (lower Aquitanian) and Miocene sediments. However, in part of the mountain SW of the Vilinska špica peak (726 m), Middle Triassic formations of the IP structural domain are brought over upper Egerian (lower Aquitanian) deposits by two NNW dipping reverse faults, with only locally preserved original depositional contact (Fig. 2). In contrast, no original depositional contacts between Cenozoic sedimentary



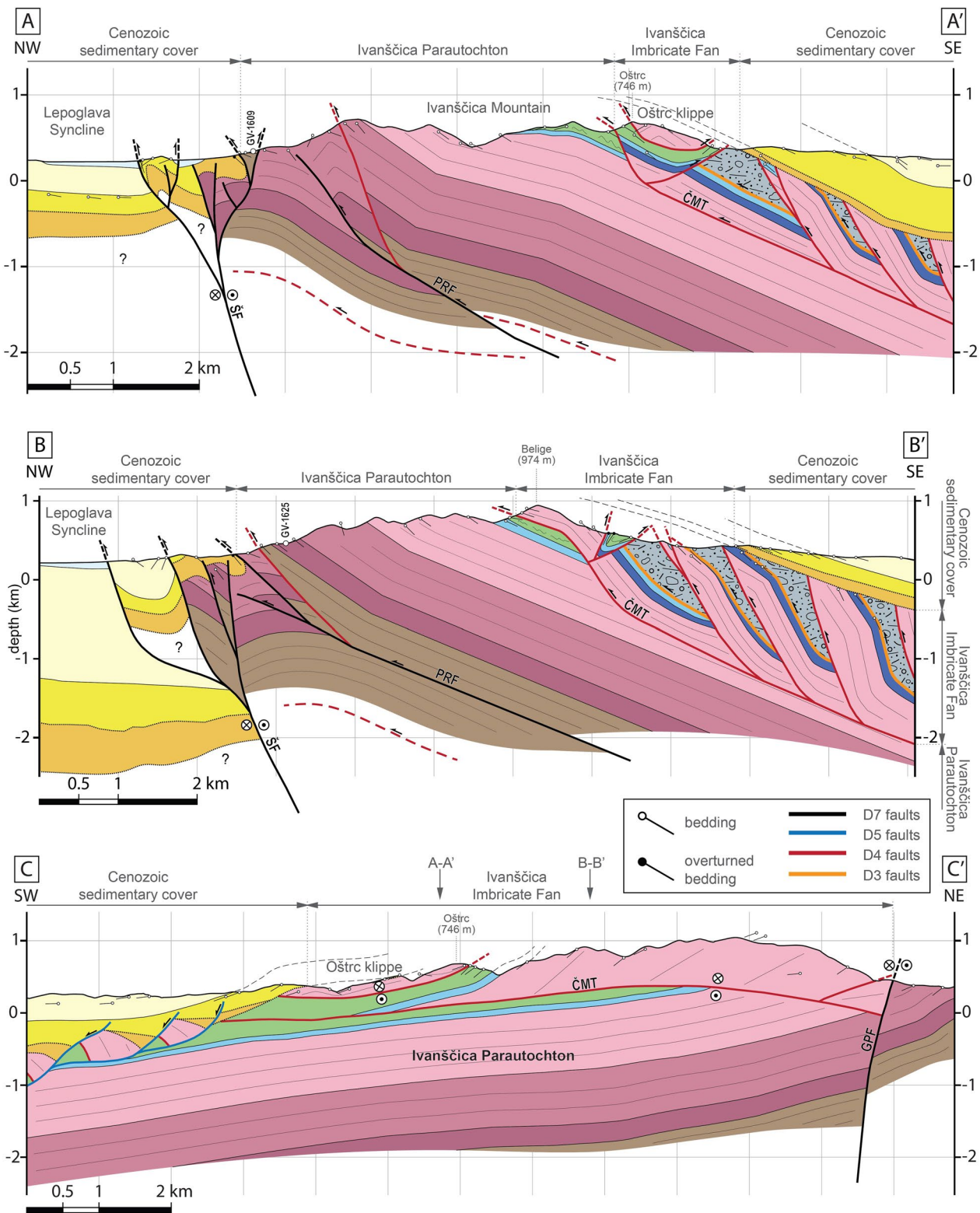


**Fig. 5** Cross-sections across Ivanščica Mt. Cross-sections **A-A'** and **B-B'** are perpendicular to the strike of structures in IIF and IP structural domains. Cross-section **C-C'** is longitudinal to the same structures. Positions of cross sections are shown in Fig. 2. For colour coding of the lithostratigraphic units, please refer to Fig. 2. ČMT Črne Mlake thrust, GPF Gotlovec-Prigorec fault, PRF Prigorec reverse fault, ŠF Šoštanj fault

cover and Permo-Mesozoic formations of the IP structural domain are preserved in the northern slopes of Ivanščica Mt. Here, Permo-Mesozoic formations of the IP structural domain are thrust northward over upper Egerian (lower Aquitanian) sediments (Figs. 2, 5). In the central part of the mountain, the well preserved Permo-Mesozoic succession dips towards S to SE below the IIF structural domain and the upper Egerian (lower Aquitanian) to Miocene cover (Fig. 5). This homoclinal structure of the IP structural domain is thrust towards NW over the rest of Permo-Mesozoic units belonging to the IP structural domain (Figs. 2, 5). These footwall units are arranged in several SE dipping imbricates and thrust NW-ward over upper Egerian (lower Aquitanian) sediments at the northern margin of the mountain (Figs. 2, 5). The youngest strata found in this homocline are Hauterivian to Albian turbidites of the Oštrc Fm. They represent the highest footwall strata overthrust by Upper Triassic to Lower Cretaceous shallow- to deep-marine sedimentary succession in a hanging wall of the SE dipping ČMT (Figs. 4, 5). The Oštrc Fm. turbidites are characterized by meter- to meso-scale tight asymmetric folds with NE trending and dominantly SW dipping fold axes (Fig. 6a, b). In the same formation, this folding is associated with an axial planar cleavage (Fig. 6a, b). Moreover, in the underlying Aptychus limestone, similar but predominantly open asymmetric folds are documented showing the same NE trending orientation of fold axes as in the overlying turbidites. Overall consistency of fold asymmetries and SE dipping axial planes and axial planar cleavage (Fig. 6a, b) with respect to the stratification, indicate NW-ward direction of tectonic transport in present-day coordinates. This is in accordance with the tectonic transport direction observed for the structurally higher IIF structural domain (see below) and the overall kinematics of the ČMT.

### 3.1.2 Ivanščica imbricate fan (IIF) structural domain

This structural domain occupies southern parts of central and eastern Ivanščica Mt. To the northwest, the domain thrusts over the IP structural domain along the SE dipping ČMT floor thrust (Figs. 2, 4 and 5). In the south, it is unconformably overlain by the upper Egerian (lower Aquitanian) and Miocene cover (Figs. 2, 4 and 5). The main structural characteristics of this domain are a series of SE dipping reverse faults splaying off the ČMT floor thrust (decollement), thus forming a stack of NW verging imbricates in their present-day orientation (Figs. 2, 5). These imbricates are made up of Upper Triassic platform carbonates, overlain by Lower Jurassic to Lower Cretaceous pelagic succession, dipping underneath the ophiolitic mélangé of the Repno Complex. The latter was previously tectonically emplaced over the pelagic Jurassic to Lower Cretaceous succession (Figs. 2, 5). Thus, the

formation of these imbricates postdates the emplacement of the ophiolitic mélangé related to the obduction of the West Vardar ophiolites (Schmid et al., 2020). The lithostratigraphic composition of the imbricates changes towards NW in that the Repno complex thrusts over progressively younger formations starting with Lower Jurassic in the SE up to lowermost Cretaceous pelagic deposits in the NW (Figs. 2, 5). The Oštrc Fm. is present only in the NW-most imbricate, locally sandwiched between the ČMT and the antithetic reverse fault named the Babin Zub back-thrust (BZBT; Figs. 2, 4, 5). The formation of the BZBT was probably favoured by a steep ramp in the SE dipping ČMT (Fig. 5). The top SE transport along the BZBT is supported by the geometry of the overturned syncline with its parasitic folds and axial planar cleavage well developed in the pelagic Aptychus limestone and the Oštrc Fm. (Figs. 5, 6d-f). Thus, the BZBT and the first imbricate to the SE form a NE striking triangle structure (Figs. 2, 5 and 6h). Within the IIF, with the exception of the Repno complex, bedding planes and axial planar cleavage prevailingly dip towards SE (Figs. 5, 6c, g). In the overturned and tight syncline formed in the hanging wall of the BZBT bedding planes and axial planar cleavage dip to the NW (Figs. 5, 6c-e).

The outcrops of the Repno complex are characterized by pervasive scaly cleavage. The planar fabric is mainly represented by clay minerals. Shaly matrix incorporates variously sized blocks of basalt, gabbro, chert, and sandstone (Fig. 7b). Basalt and gabbro blocks are usually tens and up to hundred meters in diameter, while chert and sandstone blocks are centimetre up to tens of meters in diameter. Well-developed kinematic indicators (S-C fabrics, asymmetric and symmetric boudins) record inconsistent sense of shear (Fig. 7a-c). However, close to imbricate-bounding reverse faults, kinematic indicators in the Repno complex show a sense of shear consistent with the larger scale kinematics of these faults (i.e. top NW; Fig. 7c). In the southwestern part of the IIF, the structurally highest pre-Oligo-Neogene tectonic unit, the so-called Oštrc klippe thrusts over the Oštrc Fm. of the leading imbricate (Figs. 2, 5). This klippe comprises Upper Triassic platform carbonates and subordinately Jurassic pelagic deposits, both folded in a form of NE trending anticline (Figs. 2, 5).

### 3.1.3 Cenozoic sedimentary cover (CSC)

The Cenozoic sedimentary cover unconformably overlays the Permo-Mesozoic units and seals all the older structures of the structural domains described above. Thus, the Cenozoic sediments represent the post-tectonic cover of the previously described two structural domains. This can be observed on the southern slopes of Ivanščica Mt. where none of the NW verging reverse faults in the IIF structural domain extend into the upper Egerian (lower



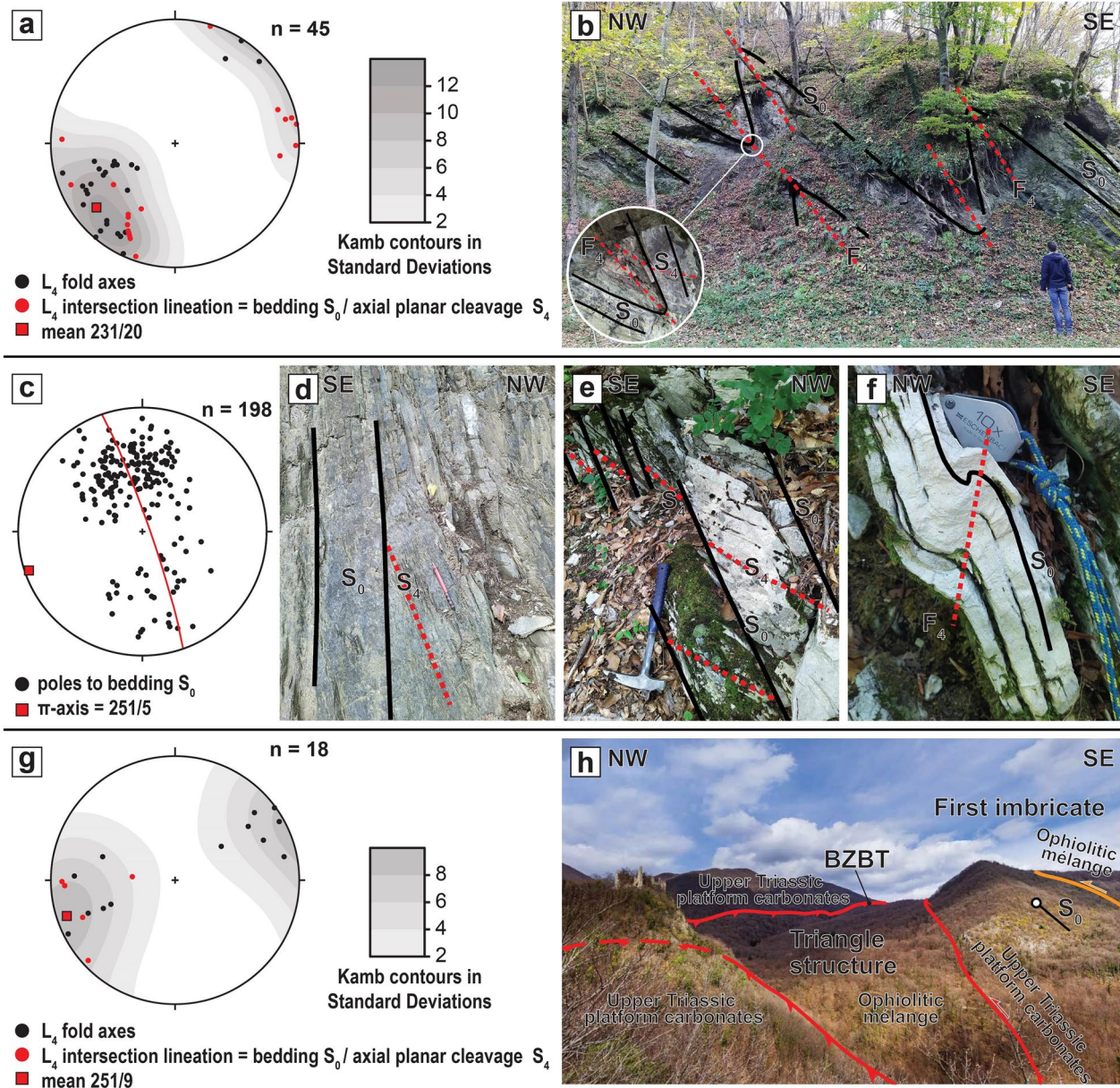


**Fig. 6** Examples of kinematic data. **a** Stereoplot of the fold axes ( $L_4$ ) and intersection lineation ( $L_4$ ) of bedding ( $S_0$ ) – axial planar cleavage ( $S_4$ ), projected on top of the Kamb contour plot. Mean orientation of the fold axes is 231/20. The measurements are taken from pelagic Aptychus limestone and Oštrc Fm. exposed within the IP structural domain. **b** Tight asymmetric folding of siltstones and calcarenites of the Lower Cretaceous Oštrc Fm. exposed within the IP structural domain (46.172552, 16.058040). **c** Stereoplot of the poles to the bedding ( $S_0$ ), best fit  $\Pi$ -circle (shown with red line) and  $\Pi$ -axis. The measurements are taken from the Upper Triassic to lowermost Cretaceous deposits exposed within the IIF structural domain. **d** Slightly overturned NE dipping bedding ( $S_0$ ) and pervasive axial planar cleavage ( $S_4$ ) within siltstones and calcarenites of the Oštrc Fm. exposed within the IIF structural domain. Outcrop is located on the NW overturned limb of the syncline in the hanging wall of the BZBT (46.166424, 16.111421; see the cross-section B-B' in Fig. 5) **e** NW dipping overturned bedding ( $S_0$ ) and pervasive axial planar cleavage ( $S_4$ ) within pelagic Aptychus limestone exposed in the IIF structural domain. Outcrop is located on the NW overturned limb of the syncline in the hanging wall of the BZBT (46.166978, 16.110589; see the cross-section B-B' in Fig. 5) **f** Second-order S-type parasitic folding of Aptychus limestone exposed within the IIF structural domain (46.164857, 16.095013). **g** Stereoplot of the fold axes ( $L_4$ ) and intersection lineation ( $L_4$ ) of bedding ( $S_0$ ) – axial planar cleavage ( $S_4$ ), projected on top of the Kamb contour plot. Mean orientation of the fold axes is 251/9. The measurements are taken from the Jurassic to lowermost Cretaceous deposits exposed within the IIF structural domain. **h** Field photo of the SE dipping imbricate, NW dipping BZBT and Triangle structure in between. See Fig. 2 for the photo location



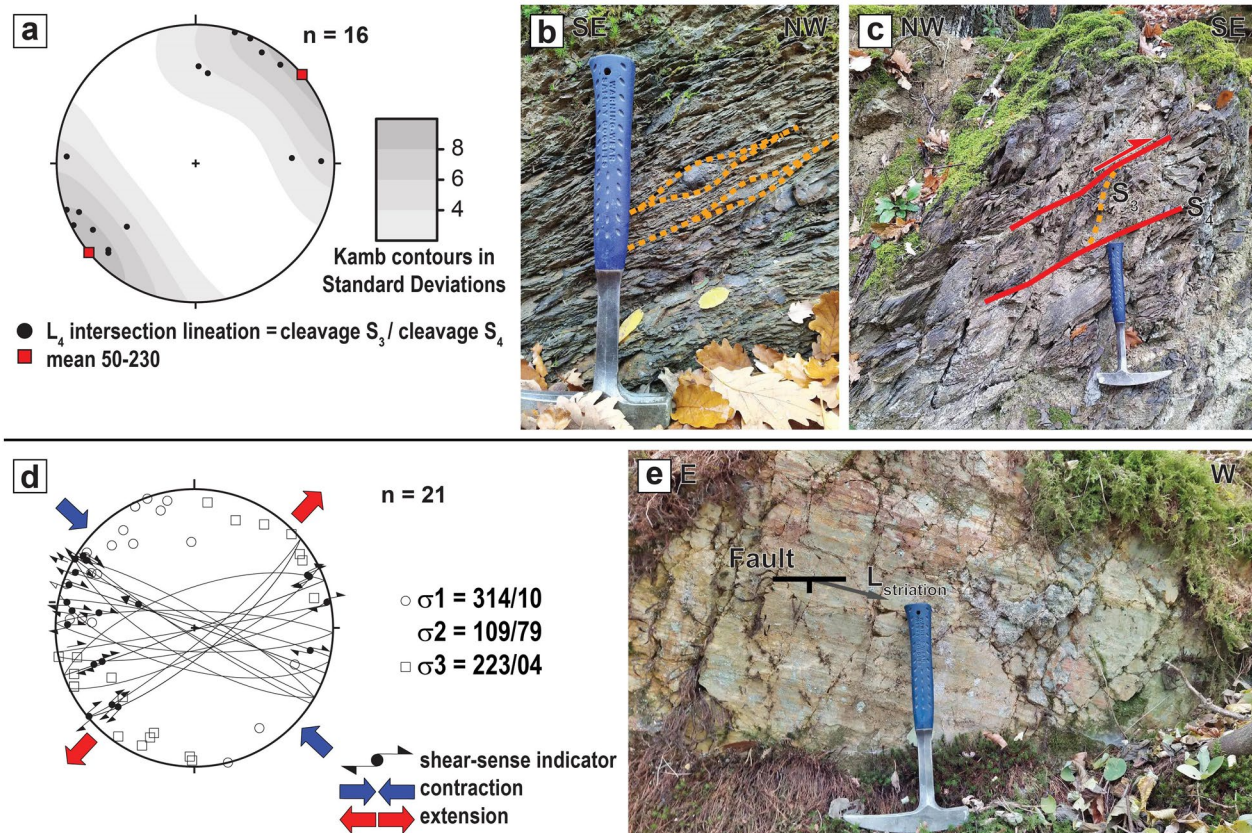


**Fig. 7** Examples of kinematic data. **a** Stereoplot of the cleavage ( $S_3$ ) – cleavage ( $S_4$ ) intersection lineation ( $L_4$ ), projected on top of the Kamb contour plot. Mean orientation of the fold axes is 50–230. The measurements are taken from the ophiolitic mélangé unit exposed within the IIF structural domain. Black poles represent intersection lineation derived from NW verging structures and red poles from SE verging structures. **b** Ophiolitic mélangé exposed within the IIF structural domain (46.156851, 16.110643) embedding deformed symmetric blocks of sandstones in a shaly matrix. **c** S-C structures in the ophiolitic mélangé exposed in the footwall just below the BZBT within the IIF structural domain (46.159118, 16.096405). **d** Stereoplot and associated paleostress tensor of strike-slip faults from the CSC. Measurements were taken along a generally ENE striking strike-slip faults to the north of Ivanščica Mt. **e** Strike-slip fault from the ENE striking dextral fault zone to the north of Ivanščica Mt. (46.219420, 16.192191), fault plane 140/82, striations 228/20, dextral displacement

Aquitania) sedimentary cover (Figs. 2, 5). Instead, the upper Egerian (lower Aquitania) sediments gently dip towards S-SE and except for this gentle tilt do not show other deformational structures. In contrast, severe tectonic deformations affecting the Cenozoic deposits are observed along the northern margin of Ivanščica Mt. where upper Egerian (lower Aquitania) sediments are overthrust by Permo-Mesozoic units of the IP structural domain along Prigorec reverse fault (PRF; Fig. 5). In addition to this, formations of the IP structural domain and the Cenozoic sedimentary cover are severely affected by transpressional faulting along a set of generally ENE striking dextral faults (Figs. 2, 5, and 7d, e). This fault set separates the Lepoglava syncline from the northwestern part of Ivanščica Mt. (see area of the left upper corner of Fig. 2) and is considered as an eastward prolongation of the dextral Šoštanj strike-slip fault (see Fig. 1c; Vrabec & Fodor, 2006; Atanackov et al., 2021). The youngest

sediments clearly affected by this dextral fault set are of late Pannonian (late Messinian) age, but younger activity cannot be excluded. Another prominent structure is the SE striking Gotalovec – Prigorec dextral strike-slip fault (GPF in Figs. 2, 4) affecting uppermost Pannonian (Fig. 2) or possibly even younger deposits. South of Ivanščica Mt., similar dextral faults are not present or only have insignificant impact on the structural setting. Here folds and minor reverse faults of E-W to NE-SW orientation are most prominent structures (Figs. 2, 7).

### 3.1.4 Oligocene-Quaternary structures in the wider study area revealed by reflection seismic data

2D reflection seismic sections and well data are used to interpret and map structures in the subsurface in order to better understand the tectonic history of the study area. Traces of used seismic sections and positions of wells are shown in Fig. 1c. Pervasive polyphase deformation



is registered across the whole study area, encompassing the entire Oligocene-Quaternary sedimentary sequence in which five characteristic types of structures were

identified: extensional listric faults, inverted extensional listric faults, folds associated with reverse faults, positive flower structures, and reverse faults (Fig. 8).

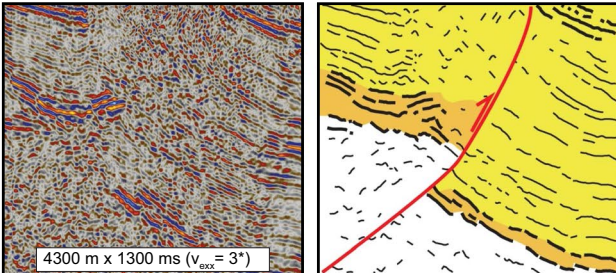
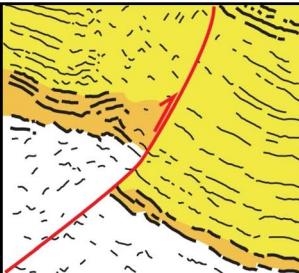
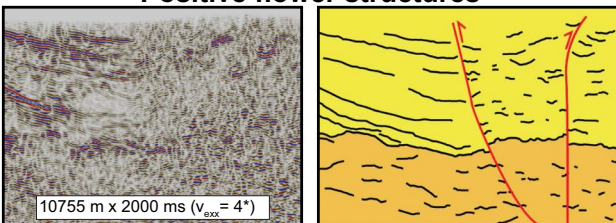
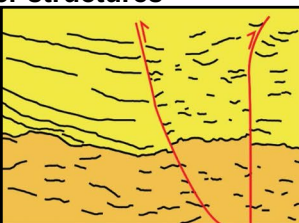
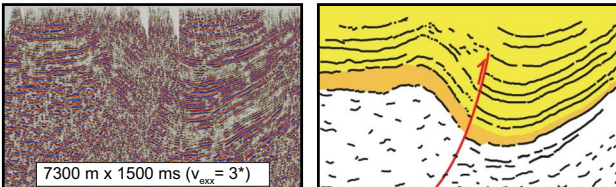
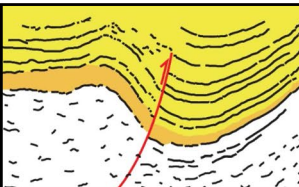
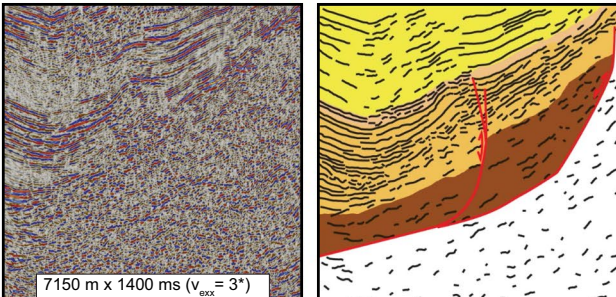
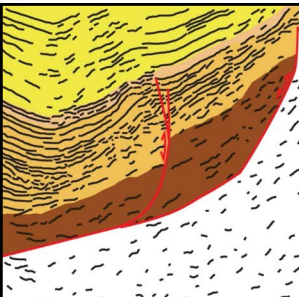
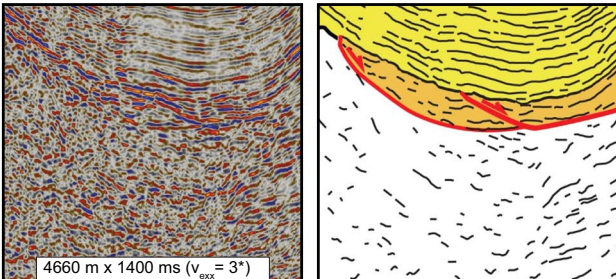
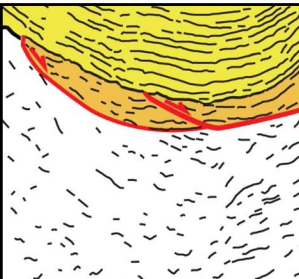
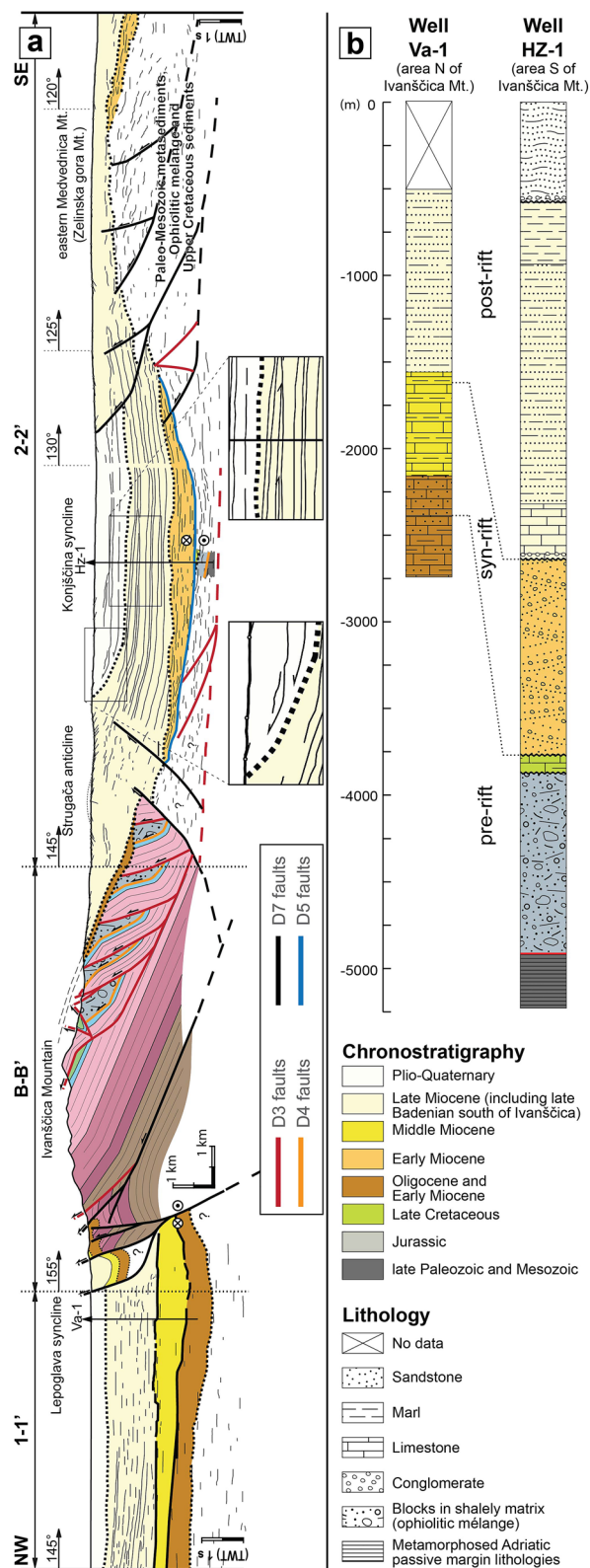
Example	Interpretation	Description of the structures
<p style="text-align: center;"><b>Reverse faults</b></p>  <p>4300 m x 1300 ms (<math>v_{\text{exx}} = 3^\circ</math>)</p>		<p><b>Deformed units:</b> whole Neogene infill  <b>Syn-tectonic units:</b> Upper Miocene (■), Pliocene-Quaternary (□)  <b>Post-tectonic units:</b> Upper Quaternary (Holocene?)  <b>Cross-cut:</b> yes, older extensional faults  <b>Reactivation:</b> no</p>
<p style="text-align: center;"><b>Positive flower structures</b></p>  <p>10755 m x 2000 ms (<math>v_{\text{exx}} = 4^\circ</math>)</p>		<p><b>Deformed units:</b> whole Neogene infill  <b>Syn-tectonic units:</b> Lower to Upper Miocene, Pliocene-Quaternary (■, ■, □)  <b>Post-tectonic units:</b> Upper Quaternary (Holocene?)  <b>Cross-cut:</b> no  <b>Reactivation:</b> no</p>
<p style="text-align: center;"><b>Reverse fault associated folds</b></p>  <p>7300 m x 1500 ms (<math>v_{\text{exx}} = 3^\circ</math>)</p>		<p><b>Deformed units:</b> whole Neogene infill  <b>Syn-tectonic units:</b> Upper Miocene (■)  <b>Post-tectonic units:</b> Upper Miocene-Pliocene, Quaternary (■, □)  <b>Cross-cut:</b> some syn-rift extensional faults  <b>Reactivation:</b> no</p>
<p style="text-align: center;"><b>Inverted extensional listric faults</b></p>  <p>7150 m x 1400 ms (<math>v_{\text{exx}} = 3^\circ</math>)</p>		<p><b>Deformed units:</b> Lower and Middle Miocene (■, ■), Upper Miocene as a drape (■)  <b>Syn-tectonic units:</b> lowermost Upper Miocene (■)  <b>Post-tectonic units:</b> Upper Miocene-Pliocene (■)  <b>Cross-cut:</b> no  <b>Reactivation:</b> no</p>
<p style="text-align: center;"><b>Extensional listric faults</b></p>  <p>4660 m x 1400 ms (<math>v_{\text{exx}} = 3^\circ</math>)</p>		<p><b>Deformed units:</b> basement units, Lower to Middle Miocene (□, ■)  <b>Syn-tectonic units:</b> Lower to Middle Miocene (■)  <b>Post-tectonic units:</b> Upper Miocene and Pliocene (■)  <b>Cross-cut:</b> no  <b>Reactivation:</b> at places as as the inverted extensional listric faults or younger reverse faults</p>

Fig. 8 Characteristic deformational structures interpreted on the seismic profiles



◀ **Fig. 9** a Regional composite cross-section composed of three segments. Segment 1-1' is located to the north of Ivanščica Mt. Note the offset between section segment 1-1' and B-B'. Segment B-B' represents the homonymous cross-section from the Fig. 5. The legend for this section is shown in Fig. 2. Segment 2-2' is located to the south of Ivanščica Mt. and ends at the easternmost slopes of Medvednica Mt. For exact location of the composite cross-section and its segments see Fig. 1c. **b** Lithostratigraphic columns of penetrated deposits from the wells Va-1 and HZ-1. For the locations of the wells see Fig. 1c. Note that the well Va-1 is not originally positioned but projected on the section segment 1-1'

The Oligocene to Middle Miocene sedimentary sequences in the research area indicate the existence of two simultaneous and contrasting paleo-environments. Specifically, during this time interval, the area north of Ivanščica Mt. was characterised by the deposition of around two kilometres thick Oligocene to Lower Miocene dominantly marine deposits (Figs. 3, 9). These deposits are cut by the Šoštanj fault and except for the upper Egerian (lower Aquitanian) deposits, do not appear south of that dextral strike-slip fault. Upper Egerian (lower Aquitanian) deposits pinch-out to the south of Ivanščica Mt., where the oldest Cenozoic deposits are of Ottnangian (middle Burdigalian) or even late Badenian (early Serravallian) age.

The syn-rift structures are the oldest Neogene structures observed in the research area. According to reflector geometry and seismic facies characteristics, it is possible to differentiate Lower to Middle Miocene syn-rift units from older basement units (Fig. 9). Inside the basement, slightly inclined to horizontal echelon zones of sub-parallel, discontinuous, high amplitude reflectors are present (Figs. 8, 9), interpreted as listric normal faults that merge in depth into a detachment dipping towards the NE. Different generations of half-grabens developed in their hanging walls are observed on seismic sections. Based on well data, half-graben formation is constrained by thick syn-rift Lower to Middle Miocene deposits (Figs. 8, 9) penetrated by the HZ-1 well (Fig. 9, see also Tomljenović & Csontos, 2001). The post-rift deposits are of late Middle Miocene and/or early Late Miocene age (Figs. 8, 9). Notably, the absence of cross-cut features indicates a coherent deformation history during Early and Middle Miocene, however, in some cases with reactivation of earlier formed normal faults, and inversion of extensional listric faults into reverse faults (Fig. 8). This tectonic inversion is coeval with Sarmatian (late Serravallian) to earliest Pannonian (early Tortonian) deposition.

Three groups of structures are observed in the deformed post-rift Upper Miocene and Pliocene deposits. The first

are reverse faults with SE and NW vergence, predominantly in the area between Ivanščica and Medvednica Mt. (Figs. 8, 9). Displacement on these faults is commonly up to hundreds of meters. As a result, the basement units are brought above Upper Miocene deposits in their footwalls. Between the Ivanščica Mt. and the Hz-1 well (Figs. 2, 9), a general vergence of these faults is towards SE, while in between this well and Medvednica Mt. reverse faults mostly dip towards SE and have NW vergence (Fig. 9). These reverse faults are usually formed as conjugate faults, and commonly bound the E-W to NE-SW striking, open and symmetric anticlines or pop-ups in their hanging walls. The most prominent structure between Ivanščica and Medvednica mountains is the Konjščina syncline (Fig. 9). In the core of this syncline 2000 m of Upper Miocene, Pliocene, and Quaternary deposits were penetrated by the Hz-1 well (Fig. 9). Onlap and downlap reflection terminations are common, but mainly connected to the syn-depositional clinoform architecture related to the basin-scale morphological shelf progradation (Fig. 9). However, the onlap features observed above the Upper Miocene clinoform unit around Hz-1 well, are folded together with the prominent reflector on which they onlap (Fig. 9). Considering the data from the Hz-1 well, this unit is represented by an alternation of sandstone and marls, which are unconformably overlain by Plio-Quaternary gravels at depth of 580 m (Fig. 9). This unconformity surface is folded and pinches out towards Strugača anticline to the N and eastern Medvednica Mt. to the S. As observed on seismic and surface structural data, the overlying Plio-Quaternary deposits are also folded and faulted (Fig. 9). The next prominent syncline is the SE trending Lepoglava syncline located to the N of Ivanščica Mt. between two regional dextral faults, the Šoštanj fault to the S and Donat fault to the N (Figs. 1, 2).

### 3.2 Apatite fission track

Apatite fission track (AFT) analyses were carried out by the Institute of Geology at Czech Academy of Sciences.

Samples for AFT analysis were collected from both Permo-Mesozoic structural domains to compare their thermal histories and reconstruct the uplift path of the Alpine—Dinaridic transitional zone. Since the study area consists mostly of carbonate sedimentary rocks and thus lacking apatite-rich lithologies, we selected the only three potentially suitable lithostratigraphic units for apatite extraction. Among overall eight samples collected from Permian to Lower Triassic sandstones, Middle Triassic volcanic rocks and Lower Cretaceous turbidites, only three samples from Permian to Lower Triassic sandstones gave enough apatites for analysis and only two of them (GV-1609 and GV-1625; Fig. 2) were successfully analysed Table 1. The apatite extraction from the rock samples (8 kg per sample) was done following standard mineral separation (REF) and their preparation for counting and subsequent measurement of uranium content by using LA-ICP-MS (Laser Ablation Inductively Coupled Plasma Mass Spectrometry) following the procedure and age calculation described by Hasebe et al. (2004). IsoplotR software (Vermeesch, 2018) and Durango apatite standard were used for zeta factor calculation and final calculation of ages.

The results of two AFT analyses are presented in Table 1. Two analysed detrital samples from the IP structural domain yield a central age of  $56.36 \pm 2.50$  Ma for GV-1609 and  $67.27 \pm 5.38$  Ma for GV-1625 (Fig. 10). Measured mean track length is  $11.12 \pm 2.54$   $\mu\text{m}$  for the sample GV-1609 and  $11.76 \pm 1.76$   $\mu\text{m}$  for the sample GV-1625. The AFT age and length measurements were combined with paleo temperature and stratigraphic constraints in order to derive the cooling trajectories for both samples by using HeFTy software based on fission track annealing algorithms (Ketcham, 2005; Ketcham et al., 2007). The obtained time–temperature model of both samples (Fig. 10) indicates fast, tectonically induced cooling that took place immediately after peak temperature conditions reached in the Early Cretaceous (ca. 140 Ma). The model suggests a drop of a temperature from a minimum 300 to 100 °C between 140 and 125 Ma

**Table 1** Apatite fission track analytical data

Sample	Lithology	Coordinates		Central age (Ma $\pm 1\sigma$ )	$N_{Gr}$	$\rho_s(N_s)$ ( $10^5 \text{ cm}^{-2}$ )	$^{238}\text{U}$ (ppm)	$2\sigma$	MSWD	P( $\chi^2$ )	Disp. (%)	Pooled age (Ma $\pm 1\sigma$ )	MTL ( $\mu\text{m} \pm \text{SD}_L$ )	$N_L$	$D_{par}$ ( $\mu\text{m}$ )
		Latitude	Longitude												
GV-1609	Upper Permian sandstone	46.20068	16.08756	$56.36 \pm 2.5$	63	0.09 (3396)	21.50	1.03	5.5	0	$28.43 \pm 3.54$		$11.12 \pm 2.54$	40	1.90
GV-1625	Lower Triassic sandstone	46.20293	16.06070	$67.27 \pm 5.38$	39	0.24 (1788)	26.90	0.99	7	0	$42.29 \pm 6.19$	$56.2 \pm 8.5$	$11.76 \pm 1.76$	37	1.74

The data presented in table are discussed in the text, see also Fig. 10.  $N_{Gr}$  number of dated apatite crystals,  $\rho_s$  spontaneous track densities,  $N_s$  sum of spontaneous fission-tracks,  $^{238}\text{U}$  mean  $^{238}\text{U}$  content value, MSWD mean square of weighted deviates, P( $\chi^2$ ) probability of obtaining chi-square ( $\chi^2$ ) for n degrees of freedom (n is the number of crystals), Disp. dispersion in single-grain ages, MTL C axis projected mean track length with  $\pm$  the standard deviation ( $\text{SD}_L$ ),  $N_L$  number of measured confined tracks,  $D_{par}$  average etch pit diameter



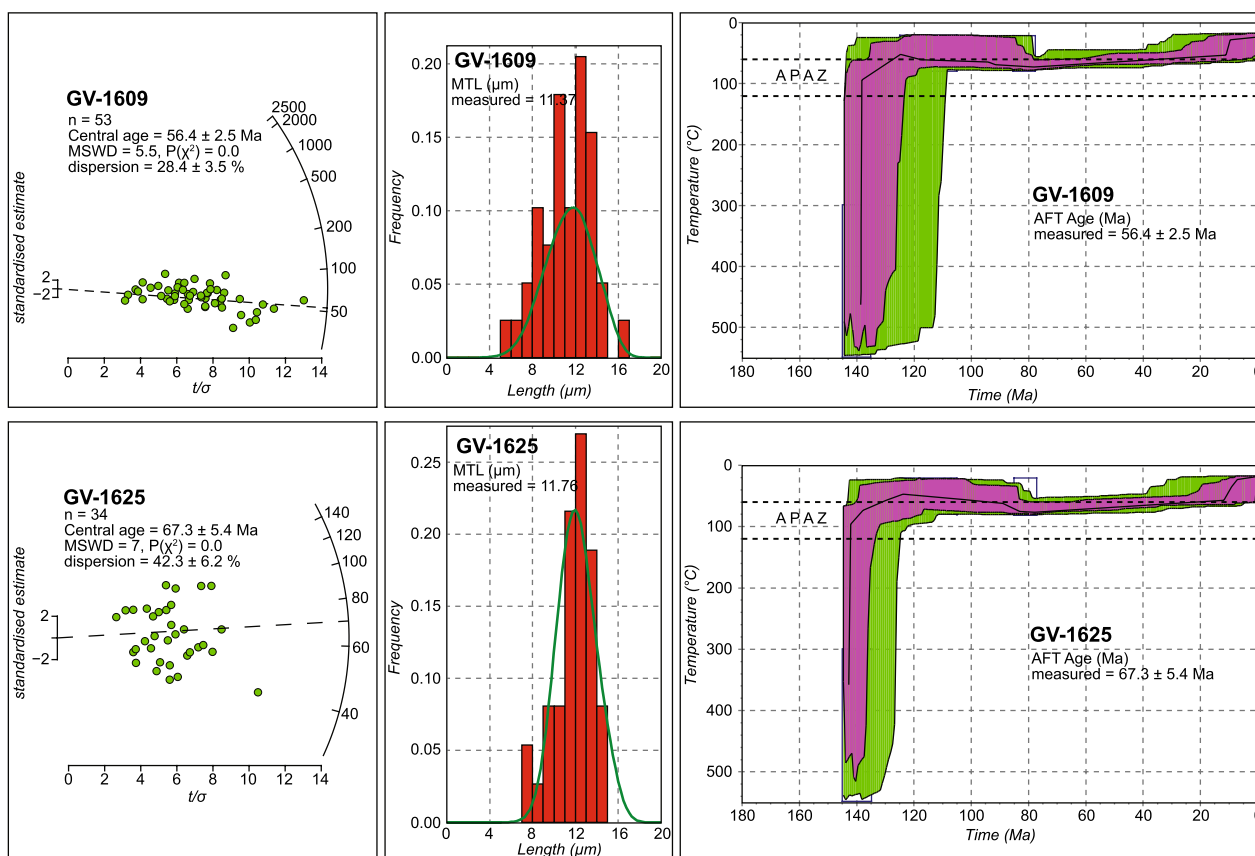


**Fig. 10** Apatite fission track data. Radial plots (plots to the left) showing the distribution of cooling ages according to the relative error and standard deviation for the apatites, accompanied by a graphs showing the distribution of the track lengths in the apatites (graphs in the middle) and a t/T graphs (graphs to the right) showing the results of HeFTy modeling based on track length and age distribution of the apatite fission tracks.  $n$  number of used data,  $MSWD$  mean square of weighted deviates,  $P(\chi^2)$  = probability of obtaining chi-square ( $\chi^2$ ) for  $n$  degrees of freedom ( $n$  is the number of crystals;  $APAZ$  apatite partial annealing zone)

and a minimum cooling rate of  $13.33$   $^{\circ}\text{C}/\text{Ma}$ . This implies denudation rate of  $0.53$   $\text{km}/\text{Ma}$  when assuming an average thermal gradient of  $25$   $^{\circ}\text{C}/\text{km}$ . The length of the apatite fission tracks corrected for the angle of measurement indicates a subsequent and relatively slow cooling period through the apatite partial annealing zone ( $APAZ$ ) followed by a stable period with only minor fluctuations around the lower temperature limit of the  $APAZ$  (Fig. 10).

### 3.3 Vitrinite reflectance

Vitrinite reflectance ( $VR$ ,  $\%R_o$ ) was measured on isolated organic matter using Zeiss Axio Imager microscope equipped with MSP 210 microscope spectrometer (oil immersion) following standard procedures (Stach et al., 1982; Taylor et al., 1998). First, total organic carbon ( $TOC$ ) content was determined on selected samples (siltstones and mudstones of Cretaceous, Jurassic, and Triassic age). The  $TOC$  content was measured on Leco C744 carbon analyser. To remove

carbonate material, samples were pre-treated with hot 18%  $\text{HCl}$ . Then, organic matter (kerogen) was isolated. Organic matter concentrate was obtained after standard  $\text{HCl}/\text{HF}/\text{ZnCl}_2$  treatment of rock. Standards used for calibration were Spinel ( $0.426\%R_o$ ), Sapphire ( $0.596\%R_o$ ), Yttrium–Aluminium–Garnet ( $0.905\%R_o$ ), Gadolinium–Gallium–Garnet ( $1.721\%R_o$ ), Cubic-Zirconia ( $3.12\%R_o$ ), Strontium–Titanate ( $5.38\%R_o$ ).  $VR$  was converted to peak paleotemperatures using formulas defined by Barker & Pawlewicz (1994) for burial heating ( $T_{\text{peak}} = (\ln R_r + 1.68)/0.0124$ ). Organic matter was examined on Olympus BX-51 microscope.

The organic matter content in the analysed siltstones and mudstones ranges from  $0.16$  to  $1.16$  wt%  $TOC$  (Table 2). Generally, organic matter content is low ( $TOC < 0.3\%$ ) except in Jurassic (GV-476) and Triassic (GT-240) siltstones ( $0.91$  and  $1.16\%$   $TOC$ , respectively). Organic matter is mainly fine detrital and of terrigenous origin, represented either with vitrinite macerals



**Table 2** Vitrinite reflectance analytical data

Sample (structural domain)	Lithology	Coordinates		TOC <sub>Leco</sub> (%)	VR %R <sub>o</sub>	No.	SD	%R <sub>min</sub>	%R <sub>max</sub>	TAI	Conversion TAI-%R <sub>o</sub>	T <sub>peak</sub> (°C)	Range T <sub>peak</sub> (°C)
		Latitude	Longitude										
GV-224 (IP)	Lower Cretaceous Siltstone	46.174581	16.066425	0.31	2.10	35	0.27	1.63	2.57	4 <sup>-</sup>	2-3	200	180-220
GV-1416 (IF)	Lower Cretaceous Siltstone	46.163606	16.093678	0.16	-					4	>3	>230	>230
GV-1633 (IF)	Lower Cretaceous Siltstone	46.162534	16.061793	0.22	2.19	24	0.21	1.80	2.54	4 <sup>-</sup>	2-3	200	190-220
DJL-8,30 (IP)	Lower Cretaceous Siltstone	46.175544	16.073502	0.20	-					4 <sup>-</sup>	2-3	>200	190-220
GV-476 (IF)	Jurassic Siltstone	46.159107	16.096391	0.91	1.81	140	0.18	1.44	2.27	3 <sup>+</sup> -4 <sup>-</sup>	1.8-2.2	185	170-200
GV-1257A (IF)	Jurassic Siltstone	46.156935	16.121706	0.27	-					4 <sup>-</sup>	2-3	>200	>200
GV-1257B (IF)	Jurassic Siltstone	46.156935	16.121706	0.21	-					4 <sup>-</sup>	2-3	>200	>200
GV-1477 (IF)	Lower Jurassic Mudstone	46.172566	16.159687	0.19	2.93	7	0.30	2.45	3.26	4 <sup>-</sup>	2-3	225	210-230
GV-1585 (IF)	Lower Jurassic Mudstone	46.174929	16.161486	0.24	1.86	5	0.07	1.76	1.95	3 <sup>+</sup> -4 <sup>-</sup>	1.8-2.2	190	180-190
MR-24,50 (IF)	Lower Jurassic Mudstone	46.164998	16.135985	0.26	1.95	45	0.53	0.92	2.80	3 <sup>+</sup> -4 <sup>-</sup>	1.8-2.2	190	135-220
GV-1113 (IP)	Middle Triassic Siltstone	46.192836	15.98391	0.40	-					4	>3	>230	>230
GT-240 (IP)	Middle Triassic Siltstone	46.181091	16.196046	1.16	3.84	31	0.42	3.05	4.71	4	>3	245	220-260

The data are discussed in the text. TOC total organic carbon, VR vitrinite reflectance, No. number of measurements, SD standard deviation;  $R_{min}$  minimum vitrinite reflectance;  $R_{max}$  maximum vitrinite reflectance, TAI thermal alteration index, IF Ivanšćica Imbricate Fan, IP Ivanšćica Parautochthon, o.m. ophiolitic mélange

or with dark, non-fluorescent, highly thermally altered amorphous organic matter. Inertinite, mainly fusinite particles are evidenced as well.

Middle Triassic organic matter is highly thermally altered. VR (3.84% $R_o$ ) corresponds to paleo-temperatures of  $\geq 245$  °C (Bostick, 1979; Barker & Pawlewicz, 1994; Rainer et al., 2016). Organic matter in Lower Jurassic mudstones is mainly amorphous while in Jurassic siltstones vitrinite macerals prevailed. VR and TAI (thermal alteration index) in all Jurassic samples indicate transition from catagenesis into metagenesis except in GV-1477 sample. VR in GV-1477 is higher (2.93% $R_o$ ) than in two others measured (1.86 and 1.95 respectively) pointing to higher paleotemperatures ( $> 225$  °C) in that sample in relation to other ones ( $\approx 190$  °C). According to VR and TAI Lower Cretaceous siltstones have reached onset of metagenesis. VR is slightly higher than 2% $R_o$ , indicating paleotemperatures  $\geq 200$  °C.

## 4 Discussion

### 4.1 Tectonic evolution of the study area and correlation with the Dinarides and the Alps

Integration of structural, AFT and VR data, together with the existing sedimentological and biostratigraphic data, enabled a reconstruction of the five deformational events that affected Permo-Mesozoic and/or Cenozoic formations of Ivanščica Mt. In addition, based on lithostratigraphic characteristics of volcano-sedimentary successions and their superposition, two older Mesozoic extensional events are also supposed. These events are discussed below in the context of the tectonic evolution of Ivanščica Mt. and in the context of the tectonic evolution of the Dinarides, Southern and Eastern Alps. The chronology of deformational events was partly derived from overprinting relations between documented deformational structures and partly based on new biostratigraphic ages of Mesozoic successions (Vukovski et al., 2023) considered as pre-, syn- and post-tectonic deposits with respect to particular deformational events. Additional time constraints were established based on AFT data.

#### 4.1.1 Pre-Cretaceous tectonic evolution

The oldest deformational event (D1 extension) on Ivanščica Mt., although not directly confirmed by deformational structures, is indicated by the presence of syn-rift volcano-sedimentary successions of Middle Triassic age. Anisian to Ladinian pelagic successions documented in the IP structural domain (Figs. 2, 3), are interpreted as having been deposited in relatively deep depocenters arranged in the form of half-grabens controlled by steep normal faults (Goričan

et al., 2005; Slovenec et al., 2020, 2023; Kukoč et al., 2023). On Ivanščica Mt., the oldest pelagic deposits are Illyrian (late Anisian) radiolarian cherts (Goričan et al., 2005; Slovenec et al., 2020; Kukoč et al., 2023), while on nearby Kuna gora Mt. ammonites from pelagic limestones indicate a Pelsonian (middle Anisian) age (Kukoč et al., 2023). Thus, according to our interpretation, this oldest deformation (D1) represents an extensional event that is related with the opening of the Neotethys Ocean during Middle Triassic times. These half-graben depocenters were short-lived, and a shallow-marine carbonate sedimentation was re-established again in the Late Ladinian (Šimunić & Šimunić, 1997; Goričan et al., 2005). Such an Anisian-Ladinian extensional event is well-documented throughout the Alps and the Dinarides, characterized by deposition of coeval and lithologically similar volcano-sedimentary successions (for correlation, see Kukoč et al., 2023).

During the Early Jurassic, after a period of Late Triassic shallow-marine sedimentation proved by Upper Triassic carbonates found in both pre-Miocene structural domains of Ivanščica Mt. (i.e., in IP and IIF structural domains), a dramatic change in depositional environments took place. In the IP structural domain, deposition of shallow-marine carbonates continued from Late Triassic into Early Jurassic until the Pliensbachian. In contrast, in the IIF structural domain the Upper Triassic shallow-marine carbonates are covered by Lower Jurassic pelagic deposits. This sharp deepening of depositional environments is assumed as related to yet another extensional event of Early Jurassic age (D2). As IP and IIF structural domains are separated by the ČMT (Figs. 2, 4 and 5), this NW verging thrust (recent orientation) is likely an inverted Early Jurassic normal fault. However, since Pliensbachian, pelagic conditions prevailed in both structural domains (Vukovski et al., 2023). This Early Jurassic extensional event correlates well with Jurassic rifting recorded in the Dinarides (Blanchet et al., 1970; Babić, 1976; Dragičević & Velić, 2002) and in the Southern and Eastern Alps, where similar lithostratigraphic successions are documented (e.g. Bertotti et al., 1993; Bohm, 2003; Goričan et al. 2012; Rožič et al., 2017). In the Alps, this Early Jurassic extension led to formation of the Alpine Tethys passive continental margin (e.g., Froitzheim & Eberli, 1990; Froitzheim & Manatschal, 1996).

#### 4.1.2 Early Cretaceous tectonic evolution

The tectonic emplacement of the Repno Complex over the stratigraphic succession of the Adriatic continental passive margin recorded in the IIF structural domain (Figs. 2, 5, 11) marks the oldest contractional event recorded on Ivanščica Mt. (D3). Age constraints for this event on Ivanščica Mt. are provided by the youngest

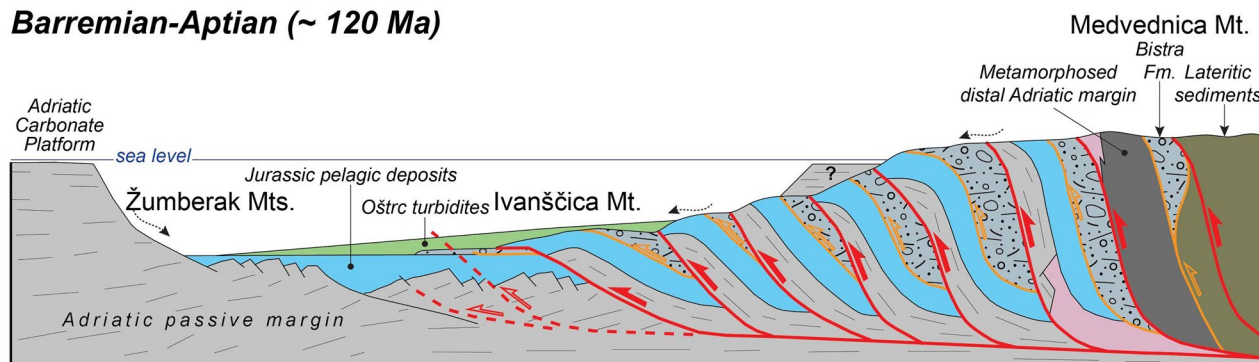
formations that are directly overthrust by the Repno Complex, which is uppermost Tithonian to Valanginian Aptychus limestone (Fig. 5). This indicates that the D3 event occurred during the Valanginian or slightly earlier.

The peak temperature conditions of approximately 200 °C recorded in the passive margin successions within the IIF structural domain (Table 2) were likely reached during this event. The obtained temperatures, calculated using the vitrinite reflection method, are only slightly higher than those estimated from the colour of pollen and dinoflagellate cysts obtained from the Repno Complex (Babić et al., 2002). This is in line with the structurally higher position of the Repno Complex with respect to the underlying passive margin successions.

Late Jurassic to earliest Cretaceous obduction of the Neotethyan ophiolites on the eastern continental margin of Adria is well documented throughout the Dinarides and the Hellenides (e.g., Bortolotti et al., 2013; Tremblay et al., 2015; Nirta et al., 2018; Schmid et al., 2020 with references). It is proposed that this obduction is responsible

for a low-grade metamorphic overprint recorded in Pale-Mesozoic units of the distal Adriatic margin underlying the ophiolites (see Fig. 11; e.g., Tomljenović et al., 2008; Porkoláb et al., 2019; Mišur et al., 2023). On Medvednica Mt., monazite dating indicates a Berriasian metamorphic event (~143 Ma; Mišur et al., 2023), while in the central Dinarides, K/Ar ages indicate Tithonian to Valanginian age of this metamorphic overprint (150–135 Ma; Porkoláb et al., 2019). Therefore, Valanginian age assumed for the D3 deformational event on Ivanščica Mt. is only slightly younger than these metamorphic ages. However, as Permian to Lower Cretaceous formations of Ivanščica Mt. are not affected by this metamorphic overprint but only a minor thermal overprint, at the time of the obduction they were in a more external (i.e., continent-ward) paleogeographic position on the Adriatic margin than units affected by this metamorphism (Fig. 11). In the central Dinarides, the youngest deposits directly overthrust by the Neotethyan ophiolites and ophiolitic mélangé have so far been described from

### Barremian-Aptian (~ 120 Ma)



### Berriasian-Valanginian (~ 140 Ma)

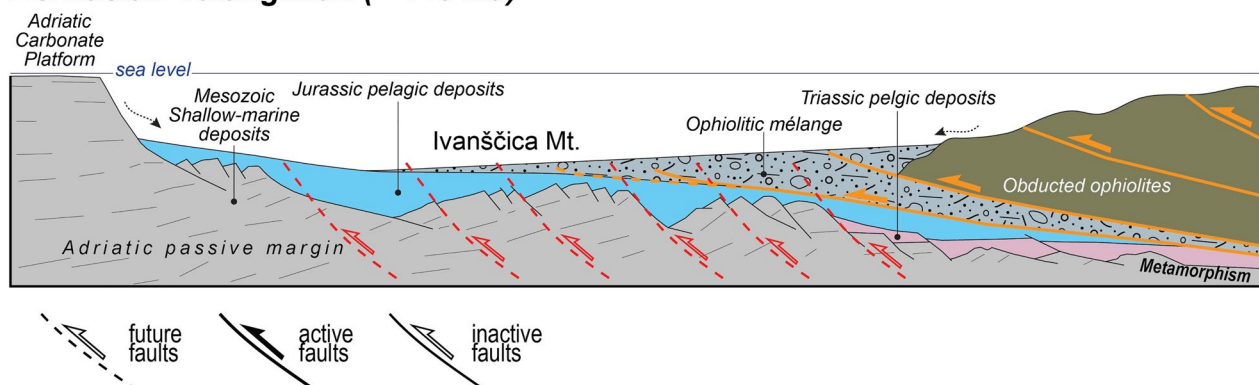


**Fig. 11** Schematic geodynamic reconstruction of the wider study area (northwesternmost Internal Dinarides) during Early Cretaceous. Different symbology is used for the faults to represent different stages in their activity as explained in the legend. Orange coloured faults were formed during D3 event related to the obduction of ophiolites and ophiolitic mélangé. D3 obduction caused metamorphism in the distal domains of the Adriatic passive margin (e.g. Medvednica Mt.), while proximal domains experienced thermal overprint. Red coloured faults were formed in subsequent D4 event and are responsible for the exhumation of Adriatic passive margin successions together with overlying ophiolitic mélangé, which enable their erosion and resedimentation within turbidites of the Oštrc Fm

the East Bosnian-Durmitor thrust sheet where the ophiolitic mélangé is found in a tectonic position above Tithonian to Berriasian pelagic limestone (Vishnevskaya et al., 2009). This limestone is correlative to the Aptychus Limestone from Ivanščica, although its age is constrained within a shorter stratigraphic range. Middle Triassic to Lower Cretaceous succession exposed on Ivanščica Mt. and attributed to the Adriatic continental margin correlate well with contemporaneous successions described from the Pre-Karst unit of the central Dinarides (Vukovski et al., 2023 with references).

Population of detrital zircons from the Oštrc Fm. with an Early Cretaceous cooling ages (ca. 145–134 Ma; Lužar-Oberiter et al., 2012) was sourced from these more internal units (e.g. Medvednica Mt.), where zircons were reset due to obduction (D3) and exhumed during subsequent D4 event.

The second contractional event recorded by deformational structures documented in the IIF and IP structural domains of Ivanščica Mt. is the D4 event. It resulted in the formation of contractional structures observed at different scales. These include NW verging imbricates of the IIF structural domain, which comprise the Repno complex and its tectonic footwall consisting of the Upper Triassic and Jurassic Adriatic passive margin succession (Figs. 5, 11). NW-ward directed thrusting of the IIF structural domain over the IP structural domain along the ČMT (Fig. 5), the formation of the BZBT (Figs. 5, 6h), NW-ward reverse faulting in the IP structural domain (Fig. 2) and intense pervasive folding of non-competent Jurassic to Lower Cretaceous pelagic deposits within both structural domains are also attributed to this deformational event (Fig. 6a–f). Sedimentological evidence supports a late Early Cretaceous age of this contractional event. The youngest deposits affected by this event are turbidites of the Hauterivian to Albian Oštrc Fm., thus indicating that this event should be at least partly post Albian in age. However, as the Oštrc Fm. contains lithoclasts of the underlying uppermost Tithonian to Valanginian Aptychus limestone (Zupanič et al., 1981), we consider this formation as syn-tectonic with respect to D4 deformational event. In addition to lithoclasts of the Aptychus limestone, the Oštrc Fm. contains other shallow-marine to pelagic lithoclasts of Triassic–Jurassic age, as well as mafic volcanic lithoclasts and abundant Cr-spinel grains (Zupanič et al., 1981). The source of all these lithoclasts and Cr-spinels is seen in the imbricates of the IIF (Figs. 5, 11). This indicates a strong, tectonically induced, fast syn-sedimentary Hauterivian to Albian exhumation and erosion of the uppermost Triassic to lowermost Cretaceous Adriatic passive margin succession together with the tectonically overlying Repno complex (Fig. 11). This is in agreement with our AFT

time–temperature models (Fig. 10) suggesting fast tectonically induced Early Cretaceous cooling and exhumation. The upper age limit of D4 event cannot be precisely constrained on Ivanščica Mt. due to the lack of post-tectonic cover deposits older than upper Egerian (lower Aquitanian). However, on the neighbouring Medvednica Mt. a correlative deformational event, D1 of van Gelder et al. (2015) or D2 of Tomljenović et al. (2008), predates the Late Cretaceous transgression and deposition of the Gosau-type sediments (Glog Fm.; Lužar-Oberiter et al., 2012 with references). Considering an Oligocene-earliest Miocene ca. 130° clockwise rotation of the block carrying Medvednica and neighbouring northern Croatian mountains (including Ivanščica) proposed by Tomljenović et al. (2008), the original trend of the D4 deformational structures documented on Ivanščica would be NW–SE and with top SW direction of tectonic transport. In that case, the initial pre-Miocene orientation and vergence of the D4 structures on Ivanščica Mt. would correspond well with contemporaneous and commonly observed SW verging structures in the Internal Dinarides (Dimitrijević, 1997; Tari, 2002; Schmid et al., 2008; Schefer, 2010; Porkoláb et al., 2019; Nirta et al., 2020).

The thermal overprint recorded in Mesozoic sediments of the IP structural domain likely reflect the D4 deformational event, since unlike the IIF structural domain, the IP was not overthrust by an ophiolitic mélangé unit. Instead, continuous sedimentation of the Oštrc Fm. on top of the Aptychus limestone is recorded in the IP structural domain (Figs. 2, 5). Therefore, we propose that peak temperature conditions in the IP structural domain were reached during D4 thrusting of the IIF structural domain over the IP, soon followed by the exhumation and cooling due to propagation of this thrusting towards the Adriatic foreland. In-sequence D4 thrusting is supported by the presence of the syn-tectonic Oštrc Fm. exclusively found in the leading sector of the IIF (Figs. 2, 5 and 11). Conodont fragments from Middle Triassic limestone exhibit CAI (conodont alteration index) value of 5–6 (Kukoč et al., 2023) corresponding to a minimum temperature of 300 °C which is slightly higher but still comparable with our VR results.

In the central Internal Dinarides, contractional deformational event correlative with the D4 documented on Ivanščica postdates the ophiolite obduction and predates the deposition of Upper Cretaceous ‘overstepping’ sequences (see in Nirta et al., 2020). Here, this event is manifested in SW-ward nappe stacking, exhumation, erosion and re-deposition of passive margin units of the distal Adriatic margin together with overlying ophiolitic units (Schmid et al., 2008; Schefer 2010; Tremblay et al., 2015; Porkolab et al., 2019; Nirta et al., 2020), also affecting the syn-orogenic turbiditic Vranduk Fm. and its proximal



equivalent the Pogari Fm. (Mikes et al., 2008; Nirta et al., 2020). These formations are correlative with syn-orogenic Hauterivian to Albian Oštrc Fm. and Aptian–Albian shallow-water Bistra Fm. (Gušić, 1975; Crnjaković, 1989; Lužar-Oberiter et al., 2012) unconformably overlying the Repno Complex in Medvednica Mt. Still, Oštrc and Bistra formations are younger than the Vranduk and Pogari formations (Mikes et al., 2008; Nirta et al., 2020 with references therein; Hrvatović, 2022), thus suggesting younger age of D4 deformations and more forelandward position of Ivanščica Mt. during this event.

In the Eastern Alps, Early Cretaceous contractional deformational event correlative with the D4 event of Ivanščica is well-known as the Eo-Alpine event characterized by WNW-ward stacking of the Austroalpine nappe units (Fig. 12; Neubauer et al., 1999; Schmid et al., 2008, 2020 and references therein) and a deposition of the syn-orogenic Rossfeld Formation of late Valanginian to Aptian age (~135–110 Ma; Faupl & Wagreich, 2000). Moreover, a regional Early Cretaceous event is documented along the whole East Alpine-Dinaridic-Hellenic belt (Neubauer et al., 1999; Schefer, 2010; Bortolotti et al., 2013), including the Western Carpathians (Plašienka et al., 1997a, b). In general, it is interpreted as related to the closure of the northern branch of the Neotethys Ocean (Fig. 12; Schmid et al., 2008; 2020; Nirta et al., 2018, 2020).

The D4 event resulted in a regional emersion recorded on Ivanščica Mt. as well as throughout the Dinarides and the Eastern Alps. The oldest sediments covering Mesozoic formations on Ivanščica Mt. are upper Egerian (lower Aquitanian) clastic deposits (Fig. 2). Locally across the Dinarides, this emersion was considerably shorter and lasted until the Late Cretaceous when ‘overstepping sediments’ were deposited on top of Mesozoic formations (Nirta et al., 2020; Hrvatović, 2022). Similarly, in the Medvednica Mt. these sediments are known as Gosau-type deposits and are of Santonian to Paleocene age (Crnjaković, 1979). Additionally, lateritic sediments on

top of serpentinites are found at the base of a Campanian rudist limestone (Palinkaš et al., 2006; Moro et al., 2010). Another evidence of emersion can be found in bauxite deposits on the neighbouring Ravna gora Mt. formed on top of Triassic dolomites, likely exhumed during the D4 event. Bauxites are sealed by upper Eocene Foraminiferal limestone (Šimunić et al., 1981; Šimunić, 1992; Čosović & Drobne, 2000). Post Early Cretaceous emersion in the study area suggests that Late Cretaceous to Eocene sedimentary burial cannot be the explanation for the thermal overprint, as it is interpreted for the area of “Sava folds” and further westward in Slovenian Basin where continuous latest Cretaceous to middle Eocene sedimentation resulted in deposition of at least 5 km of flysch type sediments (Rainer et al., 2016). Records of this emersion, which lasted from latest Jurassic to earliest Cretaceous until the Late Turonian transgression and the deposition of the Lower Gosau Group are found in the Austroalpine unit and the Western Carpathians (Wagreich & Faupl, 1994; Wagreich & Marschalko, 1995; Stern & Wagreich, 2013; Steiner et al., 2021).

The cooling trajectories of the AFT samples obtained in this study indicate a tectonically stable period with only minor fluctuations after the fast cooling related to the D4 event (Fig. 10). The central ages of  $56.4 \pm 2.5$  Ma for sample GV-1609 and  $67.3 \pm 5.4$  Ma for sample GV-1625 are the result of a long-lasting period during which these samples remained around the lower limit of the APAZ (Fig. 10). For this reason, we suppose that the IP and the IIF structural domains were not affected by any major deformation postdating D4 Early Cretaceous contraction and predating D5 Early Miocene extension.

#### 4.1.3 Neogene-recent tectonic evolution

NE dipping low angle listric normal growth faults documented on reflection seismic sections (Fig. 8), associated with ENE striking dextral strike-slip faults around the prominent Early Miocene syn-rift depocenters N of Ivanščica Mt. (Figs. 1c, 2) are attributed to the D5

(See figure on next page.)

**Fig. 12** An overview and correlation of the most important tectonic events documented on Ivanščica Mt. (Kukoč et al., 2023; Slovenec et al., 2023; Vukovski et al., 2023 and the results of this study), in the eastern Southern Alps (Doglioni & Bosellini, 1987; Castellarin et al., 1992; Doglioni, 1992; Sarti et al., 1992; Bertotti et al., 1993; Channell, 1996; Schönborn, 1999; Mandl, 2000), the Eastern Alps (Kozur, 1991; Ratschbacher et al., 1991; Schmid et al., 1996; Dunkl & Demény, 1997; Froitzheim et al., 1997; Neubauer et al., 1999; Willingshofer et al., 1999a, b; Faupl and Wagreich, 2000; Mandl, 2000; Böhm, 2003; Thöni, 2006; Gawlick et al., 2009; Missoni & Gawlick, 2011a, b; Favaro et al., 2015; Rosenberg et al., 2015; Gawlick & Missoni, 2019; Fodor et al., 2021), Dinarides (Gušić & Babić, 1970; Lanphere et al., 1975; Dragičević & Velić, 2002; Lugović et al., 2006; Schmid et al., 2008; Ustaszewski et al., 2009; Smirčić et al., 2018, 2020; Porkolab et al., 2019; van Unen et al., 2019a, b; Nirta et al., 2020; Šegvić et al., 2020; Balling et al., 2023; Slovenec & Šegvić, 2024), Pannonian Basin (Tomljenović, 2002; Tomljenović & Csontos, 2001; Horváth et al., 2006; Balázs et al., 2016) and nearby Medvednica Mt. (Tomljenović et al., 2008; van Gelder et al., 2015; Mišur et al., 2023). Note how the tectonic events are linked with the geodynamic processes within the Neotethys Ocean (Channell & Kozur, 1997; Stampfli & Borel, 2002; 2004; Schmid et al., 2004). Time scale after Cohen et al., (2013; updated). *DLS* Dinaride Lake System, *SSZ* supra subduction zone

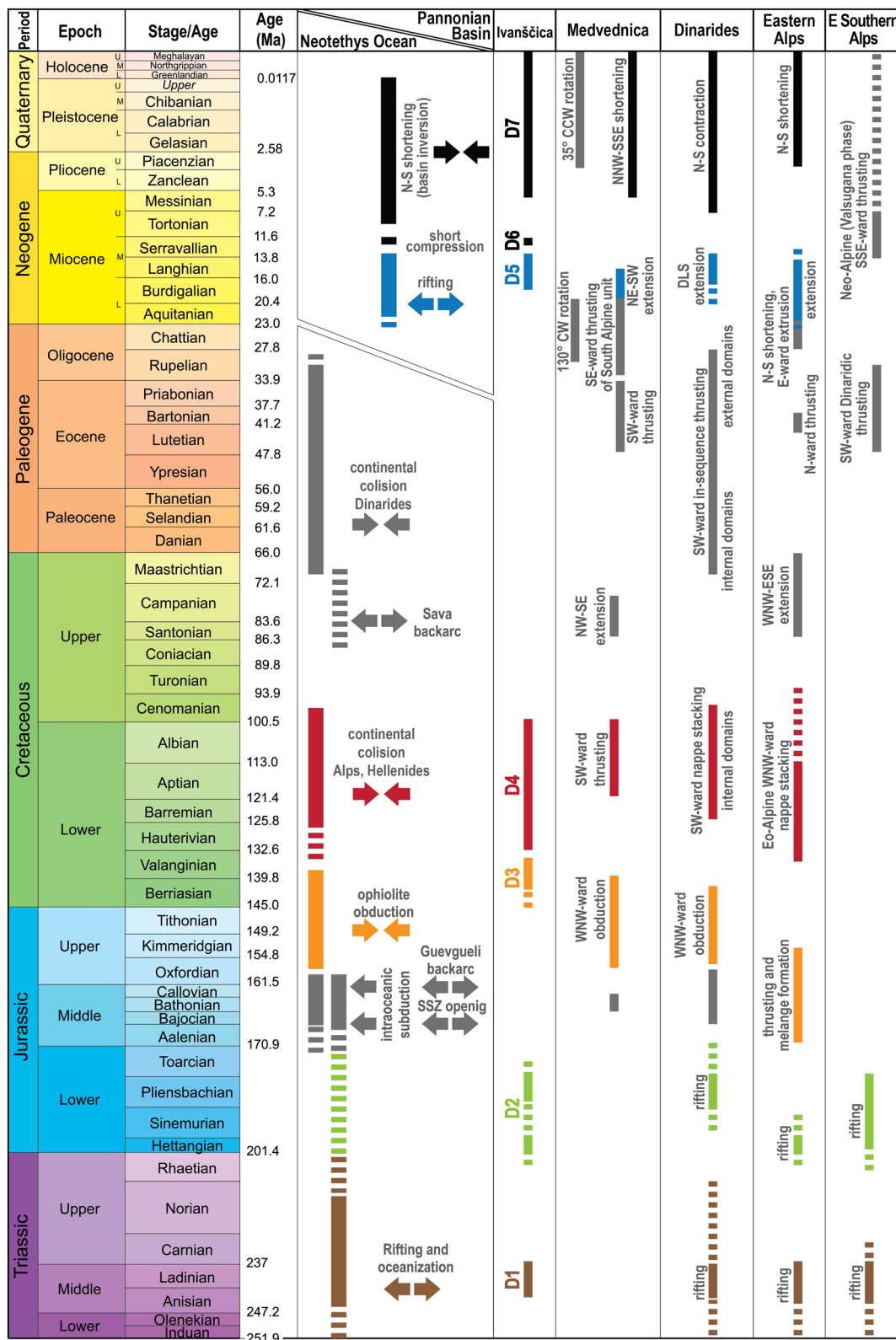


Fig. 12 (See legend on previous page.)

deformational event that resulted in Early Miocene NE-SW directed extension. The D5 normal faults cross-cut older structures (Fig. 5) with only sporadic evidence for their later inversion or reactivation. The termination of D5 extension is marked by the late Badenian (early Serravallian) transgression and deposition of clastic to carbonate sediments, which seal Early Miocene rift structures (Figs. 8, 9). The termination of this event corresponds with a gradual decrease in volcanic activity during late Middle Miocene in the Pannonian Basin (Balázs et al., 2016; Pavelić & Kovačić, 2018). Onlapping of Pannonian (Tortonian to lower Zanclean) over Sarmatian (upper Serravallian) sediments indicates a late Sarmatian (latest Serravallian) short-lived contraction (D6), also documented in reflection seismic sections near Medvednica Mt. by Tomljenović & Csontos (2001). It resulted in partial reactivation of the D5 normal listric faults into reverse faults (Fig. 8). The subsequent stage of thermal subsidence well documented across the entire Pannonian Basin area was characterised by filling of accommodation space and gradual filling of the basin during Late Miocene and Pliocene times (Kovačić et al., 2004; Sebe et al., 2020).

The youngest deformation event (D7) is of Late Miocene to recent age, and characterized by NNW-SSE contraction. To the north of Ivanščica Mt., this contraction is accommodated by the reactivation of ENE striking dextral faults (e.g. Šoštanj fault; Fig. 7d, e) and by formation of E to ENE trending km large folds and SE striking dextral faults (Fig. 2). Here, reverse faulting is mostly accommodated along local transpressional ramps of major strike-slip faults. The influence of strike-slip faulting decreases sharply to the south at the N to NW verging Prigorec reverse fault (Figs. 2, 5), which possibly represents Early Cretaceous D4 fault reactivated during D7 Late Miocene–Present contraction. This fault is responsible for NW-ward high angle thrusting of the Permo–Mesozoic units of the IP and passively transported IIF over upper Oligocene and Miocene deposits, inclination of homoclinal S to SE dipping Miocene strata in the southern slopes of the mountain (Fig. 5), and final uplift of Ivanščica. The SE striking Gotalovec – Prigorec dextral fault is attributed to the D7 event according to the late Pannonian (late Messinian) age of deformed strata. To the south and towards the Medvednica Mt., the same NNW-SSE contraction resulted in the formation of series of E to ENE trending, tens of kilometres long anticlines and synclines, with small offset reverse faults developed in the limbs of anticlines (Figs. 8, 9). Onlapping and thinning of syn-tectonic strata along the flanks of anticlines indicate that the main stage of folding started in the late Pannonian (late Messinian; Figs. 8, 9). This deformation and timing correlates well with previous field kinematic

studies and interpretations of seismic data from wider study area (Placer, 1999b; Tomljenović & Csontos, 2001; van Gelder et al., 2015; Balázs et al., 2016).

#### 4.2 Tectonic position of Ivanščica Mt.

Earlier studies considered Ivanščica, for the most part, as a S verging Neogene nappe of the South Alpine unit, thrust over the ophiolitic mélange of the Western Vardar ophiolitic unit of the Dinarides (Repno complex; Fig. 1c; Placer, 1999a; Schmid et al., 2008, 2020; van Gelder et al., 2015). Our investigation did not reveal any S to SE verging thrust of Miocene age. The only SE verging fault is the BZBT, the location and kinematics of which partially coincides with the frontal thrust of the South Alpine unit according to Placer, (1999a), van Gelder et al. (2015) and Schmid et al. (2020). However, the BZBT is sealed by upper Egerian (lower Aquitanian) deposits and thus predates Oligocene–earliest Miocene rotation. Furthermore, we interpret the BZBT to be Early Cretaceous in age (see Sect. 4.1.2.). Therefore, the initial top-NE vergence of the BZBT and its Early Cretaceous age oppose the interpretation about SE-ward Miocene thrust. In addition, the main shortening phase in the South Alpine unit (the Valsugana phase, ca. 14–8 Ma, Castellarin et al., 1992; Doglioni, 1992; Castellarin & Canteli, 2000; Zattin et al., 2003, 2006), was coeval with the regional transgression and the deposition of shallow-water to pelagic sediments in the study area (Fig. 12), including whole Pannonian Basin (Balázs et al., 2016; Pavelić & Kovačić, 2018 and references therein). However, the same driving process which caused thrusting within the South Alpine unit, the indentation and CCW rotation of Adria, is responsible for the late Pannonian (late Messinian; ~6 Ma) to recent contraction (D7). In the area of the Dinarides and the Pannonian Basin, this contraction resulted in folding, reverse and strike-slip faulting (Tomljenović & Csontos, 2001; Balázs et al., 2016; van Unen et al., 2019a, b). In contrast, at the same time the South Alpine unit was characterised by thrusting (Castellarin et al., 1992; Picotti et al., 2022). Hence, in contrast to the previous studies, our data suggest that the study area was not affected by the Miocene S-ward retro wedge thrusting characteristic for the South Alpine unit. Instead of S-ward thrusting, in the study area indentation of Adria was manifested by folding, reverse and strike-slip faulting. Considering the Mesozoic tectono-sedimentary evolution of Ivanščica Mt. (Figs. 3, 12) as described earlier in the discussion, we interpret paleogeographic affiliation of its non-ophiolitic Mesozoic structural-stratigraphic entities to the Pre-Karst unit of the Dinarides. The Repno complex belongs to the Western Vardar ophiolitic unit representing its northwesternmost outcrops. Up to now, this is the only known location where



ophiolitic mélangé of the Western Vardar ophiolitic unit is in the primary obduction thrust contact with underlying successions of the Pre-Karst unit (Figs. 5, 11).

## 5 Conclusion

Ivanščica Mt., an inselberg in the Alpine—Dinaridic transitional zone of northern Croatia, is divided into two structural domains: Ivanščica Parautochthon and Ivanščica Imbricate Fan overlain by Cenozoic sedimentary cover.

By implementation of a multi-scale structural analysis, AFT, and VR data, four contractional and one extensional event have been recorded on Ivanščica Mt. In addition, two older extensional events were recognized based on the Mesozoic tectono-sedimentary record. Middle Triassic (D1) and Early Jurassic (D2) extensional events related to the opening of the Neotethys Ocean and Alpine Tethys respectively are recorded in volcano-sedimentary successions of the IP and the IIF structural domains.

Late Berriasian to Valanginian (~140 Ma) contraction (D3) is manifested with tectonic emplacement of the ophiolitic mélangé of the Repno Complex over the stratigraphic successions of the Adriatic passive margin in the IIF structural domain and their thermal overprint.

The following contractional event (D4) was a NW-ward imbrication, thrusting of the IIF structural domain over the IP structural domain along the ČMT and thermal overprint of sedimentary succession of the IP. Syn-deformational Hauterivian to Albian Oštrc Fm. and our AFT modelling results provide age constraints for this deformational event (~133–100 Ma). When considering the post Oligo-Miocene rotations, initial NW trending and SW verging structures attributed to D4 deformational event coincide with the typical Dinaridic structural trend. This deformational event is a result of continued contraction related to the closure of the northern branch of the Neotethys Ocean and finally resulted in long lasting emersion in the Ivanščica Mt.

The youngest extensional event (D5) is characterized by formation of NE dipping predominantly listric normal faults and ENE striking dextral faults, as a consequence of ongoing extension in the Pannonian Basin. Timing of deformation is constrained by the Ottnangian (middle Burdigalian) to middle Badenian (late Langhian) age (~18–14 Ma) of syn-rift deposits observed on the reflection seismic and well data. In the early post-rift stage, short lasting late Sarmatian (late Serravallian; ~12 Ma) contraction is registered (D6), preceding the main stage of the basin inversion.

The youngest recorded deformational event (D7) characterised by late Pannonian (late Messinian; ~6 Ma) to recent NNW-SSE contraction, resulted in reactivation of

ENE striking dextral faults, formation of new SE striking dextral faults as well as the formation of E to ENE trending folds and reverse faults. This event is a result of the N-ward indentation and CCW rotation of the Adriatic microplate. Overall Miocene and post-Miocene deformation history of the study area is in agreement with well-known Pannonian back-arc tectonics starting in the Early Miocene.

Our results infer that the study area was affected by tectonic processes related to the different stages of the evolution of the Neotethys Ocean, opening of the Alpine Tethys Ocean, as well as the opening and inversion of the Pannonian Basin. Mesozoic tectono-sedimentary evolution of Ivanščica Mt. proves the paleogeographic affiliation of its non-ophiolitic Mesozoic structural-stratigraphic entities to the Pre-Karst unit of the Dinarides.

## Abbreviations

AFT	Apatite fission track
APAZ	Apatite partial annealing zone
BZBT	Babin Zub back-thrust
CCW	Counter clockwise
CSCW	Cenozoic sedimentary cover
ČMT	Črne Mlake thrust
Dn	Deformational event (n is the number indicating the relative age of the event where the number 1 is the oldest event)
DLS	Dinaride Lake System
GPF	Gotalovec-Prigorec fault
IIF	Ivanščica Imbricate Fan
IP	Ivanščica Parautochthon
MSWD	Mean square of weighted deviates
n	Number of used data
PRF	Prigorec reverse fault
P( $\chi^2$ )	Probability of obtaining chi-square ( $\chi^2$ ) for n degrees of freedom (n is the number of crystals)
SSZ	Supra subduction zone
ŠF	Šoštanj fault
TAI	Thermal alteration index
VR	Vitrinite reflectance

## Acknowledgements

László Csontos (MOL Group) and Michele Marroni (Università di Pisa) are gratefully acknowledged for their reviews and suggestions that have significantly improved the first version of the manuscript. The authors would like to thank to Matija Šimunić for providing the photo in Fig. 6h. The authors are especially grateful to the editors Daniel Marty (Naturhistorisches Museum Basel) and Stefan M. Schmid (Universität Basel) for coordinating the publishing process and additional and very helpful comments and suggestions by Stefan M. Schmid. This research was supported by the Croatian Science Foundation under the project "Revealing the Middle Triassic Paleotethyan Geodynamics Recorded in the Volcano-Sedimentary Successions of NW Croatia (GOST)" (IP-2019-04-3824).

## Author contributions

Matija Vukovski: conceptualization, methodology, field work (lead), analysis (structural), investigation, writing—original draft, review and editing (lead); Marko Špelić: analysis (seismic sections), writing—original draft, review and editing (equal); Duje Kukoč: field work (supporting), writing—original draft, review and editing (equal); Tamara Troskot-Čorbić: analysis (vitrinite reflectance), writing—original draft, review and editing (equal); Tonči Grgasović: field work (supporting), writing—review and editing (supporting); Damir Slovenec: writing—review and editing (supporting); Bruno Tomljenović: conceptualization, methodology, field work (supporting), writing—original draft, review and editing (supporting).

**Funding**

This research was funded by the Croatian Science Foundation under the project “Revealing the Middle Triassic Paleotethyan Geodynamics Recorded in the Volcano-Sedimentary Successions of NW Croatia (GOST)” (IP-2019-04-3824).

**Data availability**

All data generated or analysed during this study are included in this article.

**Declarations****Competing interests**

The authors have no competing interests to declare that are relevant to the content of this article.

**Author details**

<sup>1</sup>Croatian Geological Survey, Sachsova 2, 10000 Zagreb, Croatia. <sup>2</sup>INA -Oil Company, Plc., Exploration & Production, E&P Laboratory, Lovinčeva 4, 10000 Zagreb, Croatia. <sup>3</sup>Faculty of Mining, Geology and Petroleum Engineering, University of Zagreb, Pierottijeva 6, 10000 Zagreb, Croatia.

Received: 26 February 2024 Accepted: 13 June 2024

Published online: 02 September 2024

**References**

- Aničić, B. & Juriša, M. (1984). Osnovna geološka karta SFRJ 1:100,000, list Rogatec L33–68 (Basic Geological Map of SFRY 1:100,000, Rogatec sheet). Geološki zavod Ljubljana and Geološki zavod Zagreb, Savezni geološki zavod.
- Atanackov, J., Jamšek Rupnik, P., Jež, J., Celarc, B., Novak, M., Milanič, B., Markelj, A., Bavec, M. & Kastelic, V. (2021). Database of active faults in Slovenia: Compiling a new active fault database at the junction between the Alps, the Dinarides and the Pannonian Basin Tectonic Domains. *Frontiers in Earth Science*, 9, 604388. <https://doi.org/10.3389/feart.2021.604388>.
- Avanić, R., Pavelić, D., Pécskay, Z., Miknić, M., Tibljaš, D., & Wacha, L. (2021). Tidal deposits in the Early Miocene Central Paratethys: The Vučji Jarek and Čemernica members of the Macelj formation (NW Croatia). *Geologia Croatica*, 74, 41–56.
- Babić, Lj. (1974). Jurassic-Cretaceous sequence of Mt Ivanščica (Northern Croatia). *Bulletin Scientifique Conseil Des Académies Des Sciences Yougoslavie*, 19(7–8), 181–182.
- Babić, Lj. (1976). Pomak granice između unutrašnje i vanjske Dinarske regije, primjer šireg područja Žumberka (Migration of the boundary between “inner” and “outer” Dinaric zones). *The 8th Yugoslavian Geological Congress*, 2, 45–51.
- Babić, Lj., Hochuli, P. A., & Zupanić, J. (2002). The Jurassic ophiolitic mélange in the NE Dinarides: Dating, internal structure and geotectonic implications. *Eclogae Geologicae Helveticae*, 95, 263–275.
- Babić, Lj., & Zupanić, J. (1973). Uppermost Jurassic and Early Cretaceous deposits on Mt. Ivanščica—northern Croatia. *Geološki Vjesnik*, 26, 267–272.
- Babić, Lj., & Zupanić, J. (1978). Mlađi mezozoik Ivanščice. In Lj. Babić & V. Jelaska (Eds.), *Vodič ekskurzije 3. Skupa sedimentologa Jugoslavije* (pp. 11–23). Zagreb: Croatian Geological Society.
- Balázs, A., Matenco, L., Magyar, I., Horváth, F., & Cloetingh, S. (2016). The link between tectonics and sedimentation in back-arc basins: New genetic constraints from the analysis of the Pannonian Basin. *Tectonics*, 35(6), 1526–1559.
- Balling, P., Tomljenović, B., Herak, M., & Ustaszewski, K. (2023). Impact of mechanical stratigraphy on deformation style and distribution of seismicity in the central External Dinarides: A 2D forward kinematic modelling study. *Swiss Journal of Geosciences*, 116, 7.
- Barker, C. E., & Pawlewicz, M. J., et al. (1994). Calculation of vitrinite reflectance from thermal histories and peak temperatures a comparison of methods. In P. Mukhopadhyay (Ed.), *Vitrinite reflectance as a maturity parameter. ACS Symposium Series* (pp. 216–229). American Chemical Society.
- Basch, O. (1981). Osnovna geološka karta SFRJ 1:100,000, list Ivanić-Grad L33–81 (Basic Geological Map of SFRY 1:100,000, Ivanić-Grad sheet). Geološki zavod Zagreb, Savezni geološki zavod.
- Belak, M., Slovenec, D., Kolar Jurkovšek, T., Garašić, V., Pécskay, Z., Tibljaš, D., & Mišur, I. (2022). Low-grade metamorphic rocks of the Tethys subduction–collision zone in the Medvednica Mt. (NW Croatia). *Geologica Carpathica*, 73(3), 207–229.
- Belak, M., & Tibljaš, D. (1998). Discovery of blueschists in the Medvednica Mountain (Northern Croatia) and their significance for the interpretation of the geotectonic evolution of the area. *Geologia Croatica*, 51(1), 27–32.
- Bertotti, G., Picotti, V., Bernoulli, D., & Castellarin, A. (1993). From rifting to drifting: Tectonic evolution of the South-Alpine upper crust from the Triassic to the Early Cretaceous. *Sedimentary Geology*, 86, 53–76.
- Blanchet, R., Cadet, J.-P., & Charvet, J. (1970). Sur l'existence d'unités intermédiaires entre la zone du Haut-Karst et l'unité du flysch bosniaque, en Yougoslavie; la sous-zone prekarstique. *Bulletin De La Société Géologique De France*, 57-XII(2), 227–236.
- Böhm, F. (2003). Lithostratigraphy of the Adnet Group (Lower to Middle Jurassic, Salzburg, Austria). In W. E. Piller (Ed.), *Stratigraphia Austriaca—Österr Akad Wiss Schriften Erdwiss Komm* (Vol. 16, pp. 231–268). VÖAW.
- Bortolotti, V., Chiari, M., Marroni, M., Pandolfi, L., Principi, G., & Saccani, E. (2013). Geodynamic evolution of ophiolites from Albania and Greece (Dinaric–Hellenic belt): One, two, or more oceanic basins? *International Journal of Earth Sciences*, 102, 783–811.
- Bostick, N. H. (1979). Microscopic measurements of the level of catagenesis of solid organic matter in sedimentary rocks to aid exploration for petroleum and to determine former burial temperatures—A review. *SEPM, Special Publication*, 26, 17–43.
- Buser, S. (1977). Osnovna geološka karta SFRJ 1:100,000, list Celje L33–67 (Basic Geological Map of SFRY 1:100,000, Celje sheet). Geološki zavod Ljubljana, Savezni geološki zavod.
- Castellarin, A., & Cantelli, L. (2000). Neo-Alpine evolution of the Southern Eastern Alps. *Journal of Geodynamics*, 30, 251–274.
- Castellarin, A., Cantelli, L., Fesce, A. M., Mercier, J. L., Picotti, V., Pini, G. A., Prosser, G., & Selli, L. (1992). Alpine compressional tectonics in the Southern Alps. Relationships with the N-Apennines. *Annales Tectonicae*, 6(1), 62–94.
- Channell, J. E. T. (1996). Palaeomagnetism and palaeogeography of Adria. *Geological Society, London, Special Publications*, 105(1), 119–132.
- Channell, J. E. T., & Kozur, H. W. (1997). How many oceans? Meliata, Vardar, and Pindos oceans in Mesozoic Alpine palaeogeography. *Geology*, 25, 183–186.
- Cohen, K. M., Finney, S. C., Gibbard, P. L., & Fan, J.-X. (2013). The ICS International Chronostratigraphic Chart. *Episodes*, 36, 199–204.
- Ćosović, V., & Drobne, K. (2000). Some remarks on Nummulites specimens from localities in south-eastern Slovenia and north-western Croatia. In D. Bassi (Ed.), *Shallow water benthic communities at the Middle-Upper Eocene boundary (Southern and north-eastern Italy, Slovenia, Croatia, Hungary)* (pp. 14–15). Annali dell'Università di Ferrara.
- Crnjaković, M. (1979). Sedimentation of transgressive Senonian in Southern Mt. Medvednica [In Croatian with English summary]. *Geološki Vjesnik*, 32, 81–95.
- Crnjaković, M. (1989). Lower Cretaceous shallow marine deposits in Mt. Medvednica [In Croatian with English summary]. *Acta Geologica Zagreb*, 19, 61–93.
- Dimitrijević, M. D. (1997). *Geology of Yugoslavia* (2nd ed.). Geoinstitute.
- Dogliani, C. (1992). Relationships between Mesozoic extensional tectonics, stratigraphy and Alpine inversion in the Southern Alps. *Eclogae Geologicae Helveticae*, 85, 105–126.
- Dogliani, C., & Bosellini, A. (1987). Eoalpine and mesoalpine tectonics in the Southern Alps. *Geologische Rundschau*, 76, 735–754.
- Dogliani, C., Harabaglia, P., Merlini, S., Mongelli, F., Peccerillo, A., & Piromallo, C. (1999). Orogens and slabs vs their direction of subduction. *Earth Science Reviews*, 45(3–4), 167–208.
- Dragičević, I., & Velić, I. (2002). The northeastern margin of the Adriatic Carbonate Platform. *Geologia Croatica*, 55(2), 185–232.
- Dunkl, I., & Demény, A. (1997). Exhumation of the Rechnitz Window at the border of the Eastern Alps and Pannonian Basin during Neogene extension. *Tectonophysics*, 272(2–4), 197–211.
- Faccenna, C., Becker, T. W., Conrad, C. P., & Husson, L. (2013). Mountain building and mantle dynamics. *Tectonics*, 32, 1–15.

- Faccenna, C., Piromallo, C., Crespo-Blanc, A., Jolivet, L., & Rosetti, F. (2004). Lateral slab deformation and the origin of the western Mediterranean arcs. *Tectonics*. <https://doi.org/10.1029/2002TC001488>
- Faupl, P., & Wagreich, M. (2000). Late Jurassic to Eocene palaeogeography and geodynamic evolution of the Eastern Alps. *Mitteilungen der Österreichischen Geologischen Gesellschaft*, 92, 79–94.
- Favaro, S., Schuster, R., Handy, A., Scharf, A., & Pestal, G. (2015). Transition from orogen-perpendicular to orogen-parallel exhumation and cooling during crustal indentation—Key constraints from  $147\text{Sm}/144\text{Nd}$  and  $87\text{Rb}/87\text{Sr}$  geochronology (Tauern Window, Alps). *Tectonophysics*, 665, 1–16.
- Fodor, L., Balázs, A., Csillag, G., Dunkl, I., Héja, G., Jelen, B., Kelemen, P., Kövér, S., Németh, A., Nyíri, D., Selmecci, I., Trajanova, M., Vrabec, M., & Vrabec, M. (2021). Crustal exhumation and depocenter migration from the Alpine orogenic margin towards the Pannonian extensional back-arc basin controlled by inheritance. *Global and Planetary Change*. <https://doi.org/10.1016/j.gloplacha.2021.103475>
- Fodor, L., Jelen, B., Márton, E., Skaberne, D., Car, J., & Vrabec, M. (1998). Miocene-Pliocene tectonic evolution of the Slovenian Periadriatic fault: Implications for Alpine-Carpathian extrusion models. *Tectonics*, 17(5), 690–709.
- Froitzheim, N., Conti, P., & van Daalen, M. (1997). Late Cretaceous, synorogenic, low-angle normal faulting along the Schling fault (Switzerland, Italy, Austria) and its significance for the tectonics of the Eastern Alps. *Tectonophysics*, 280(3–4), 267–293.
- Froitzheim, N., & Eberli, G. P. (1990). Extensional detachment faulting in the evolution of a Tethys passive continental margin, Eastern Alps, Switzerland. *Geological Society of America Bulletin*, 102(9), 1297–1308.
- Froitzheim, N., & Manatschal, G. (1996). Kinematics of Jurassic rifting, mantle exhumation, and passive-margin formation in the Austroalpine and Penninic nappes (eastern Switzerland). *Bulletin of the Geological Society of America*, 108, 1120–1133.
- Gawlick, H. J., & Missoni, S. (2019). Middle-Late Jurassic sedimentary mélange formation related to ophiolite obduction in the Alpine-Carpathian-Dinaridic Mountain Range. *Gondwana Research*, 74, 144–172.
- Gawlick, H. J., Missoni, S., Schlagintweit, F., Suzuki, H., Frisch, W., Krystyn, L., Blau, J., & Lein, R. (2009). Jurassic Tectonostratigraphy of the Austroalpine domain. *Journal of Alpine Geology*, 50(1), 1–152.
- Goričan, Š., Halamić, J., Grgasović, T., & Kolar-Jurkovšek, T. (2005). Stratigraphic evolution of Triassic arc-backarc system in northwestern Croatia. *Bulletin De La Société Géologique De France*, 176(1), 3–22.
- Goričan, Š., Košir, A., Rožič, B., Šmuc, A., Gale, L., Kukoč, D., Celarc, B., Črne, A. E., Kolar-Jurkovšek, T., Placer, L., & Skaberne, D. (2012). Mesozoic deep-water basins of the eastern Southern Alps (NW Slovenia). *Journal of Alpine Geology*, 54, 101–143.
- Gušić, I. (1975). Lower Cretaceous imperforate Foraminifera of Mt. Medvednica, Northern Croatia (Families: Litoullidae, Ataxophragmidiidae, Orbitolinidae). *Paleontologica Jugoslavica*, 14, 7–48.
- Gušić, I., & Babić, Lj. (1970). Neke biostratigrafske i litogenetske osobine jure Žumberka. *Geološki Vjesnik*, 23, 39–49.
- Haas, J., Mioč, P., Pamić, J., Tomljenović, B., Arkai, P., Berczi-Makk, A., Koroknai, B., Kovács, S., & Felgenhauer, E. R. (2000). Complex structural pattern of the Alpine-Dinaridic-Pannonian triple junction. *International Journal of Earth Sciences*, 89, 377–389.
- Halamić, J., Goričan, Š., Slovenec, D., & Kolar-Jurkovšek, T. (1999). A Middle Jurassic Radiolarite-Clastic Succession from the Medvednica Mt. (NW Croatia). *Geologia Croatica*, 52(1), 29–57.
- Halamić, J., Marchig, V., & Goričan, Š. (2005). Jurassic radiolarian cherts in northwestern Croatia: Geochemistry, material provenance and depositional environment. *Geologica Carpathica*, 56(2), 123–136.
- Hasebe, N., Barbarand, J., Jarvis, K., Carter, A., & Hurford, A. J. (2004). Apatite fission track chronometry using laser ablation ICP-MS. *Chemical Geology*, 207, 135–145.
- Horváth, F., Bada, G., Szaifán, P., Tari, G., Ádám, A., & Cloetingh, S. (2006). Formation and deformation of the Pannonian Basin: Constraints from observational data. *Geological Society London Memoirs*, 32(1), 191–206.
- Hrvatović, H. (2022). *Geološki vodič kroz Bosnu i Hercegovinu*. Akademija nauka i umjetnosti Bosne i Hercegovine.
- Jolivet, L., & Faccenna, C. (2000). Mediterranean extension and the Africa-Eurasia collision. *Tectonics*, 19(6), 1095–1106.
- Judik, K., Rantitsch, G., Rainer, T. M., Arkai, P., & Tomljenović, B. (2008). Alpine metamorphism of organic matter in metasedimentary rocks from Mt. Medvednica (Croatia). *Swiss Journal of Geosciences*, 101, 605–616.
- Ketcham, R. A. (2005). Forward and inverse modeling of low-temperature thermochronometry data. *Reviews in Mineralogy and Geochemistry*, 58(1), 275–314.
- Ketcham, R. A., Carter, A., Donelick, R. A., Barbarand, J., & Hurford, A. J. (2007). Improved modeling of fission-track annealing in apatite. *American Mineralogist*, 92(5–6), 799–810.
- Kissling, E., Schmid, S. M., Lippitsch, R., Ansgor, J., & Fügenschuh, B. (2006). Lithosphere structure and tectonic evolution of the Alpine arc: New evidence from high-resolution teleseismic tomography. *Geological Society, London, Memoirs*, 32(1), 129–145.
- Kovačić, M., Zupanić, J., Babić, Lj., Vrsaljko, D., Miknić, M., Bakrač, K., Hećimović, I., Avanić, R., & Brkić, M. (2004). Lacustrine basin to delta evolution in the Zagorje Basin, a Pannonian sub-basin (Late Miocene: Pontian, NW Croatia). *Facies*, 50, 19–33.
- Kozur, H. (1991). The evolution of the Meliata-Hallstatt ocean and its significance for the early evolution of the Eastern Alps and western Carpathians. *Palaeogeography Palaeoclimatology Palaeoecology*, 87, 109–135.
- Kukoč, D., Slovenec, D., Šegvić, B., Vukovski, M., Belak, M., Grgasović, T., Horvat, M., & Smirčić, D. (2024). The early history of the Neotethys archived in the ophiolitic mélange of northwestern Croatia. *Journal of the Geological Society*. <https://doi.org/10.1144/jgs2023-143>
- Kukoč, D., Smirčić, D., Grgasović, T., Horvat, M., Belak, M., Japundžić, D., Kolar-Jurkovšek, T., Šegvić, B., Badurina, L., Vukovski, M., & Slovenec, D. (2023). Biostratigraphy and facies description of Middle triassic rift-related volcano-sedimentary successions at the junction of the Southern Alps and the Dinarides (NW Croatia). *International Journal of Earth Sciences*, 112, 1175–1291.
- Lanphere, M., Coleman, R. G., Karamata, S., & Pamić, J. (1975). Age of amphibolites associated with Alpine peridotites in the Dinaride ophiolite zone, Yugoslavia. *Earth and Planetary Science Letters*, 26, 271–276.
- Lugović, B., Šegvić, B., Babajić, E., & Trubelj, F. (2006). Evidence for short-living intraoceanic subduction in the Central Dinarides, Konjuh Ophiolite Complex (Bosnia–Herzegovina). International Symposium on the Mesozoic Ophiolite Belts of the Northern Part of the Balkan Peninsula. Serbian Academy of Sciences and Arts, Committee of Geodynamics, Belgrade, pp. 72–75. May 31st–June 6th, 2006.
- Lugović, B., Slovenec, D., Halamić, J., & Altherr, R. (2007). Petrology, geochemistry and geotectonic affinity of the Mesozoic ultramafic rocks from the southwesternmost Mid-Transdanubian Zone in Croatia. *Geologica Carpathica*, 58(6), 511–530.
- Lužar-Oberiter, B., Mikes, T., Dunkl, I., Babić, Lj., & von Eynatten, H. (2012). Provenance of cretaceous synorogenic sediments from the NW Dinarides (Croatia). *Swiss Journal of Geosciences*, 105, 377–399.
- Lužar-Oberiter, B., Mikes, T., von Eynatten, H., & Babić, Lj. (2009). Ophiolitic detritus in Cretaceous clastic formations of the Dinarides (NW Croatia): Evidence from Cr-spinel chemistry. *International Journal of Earth Sciences*, 98, 1097–1108.
- Magyar, I., Radivojević, D., Sztanó, O., Synak, R., Ujszászi, K., & Pócsik, M. (2013). Progradation of the paleo-Danube shelf margin across the Pannonian Basin during the Late Miocene and Early Pliocene. *Global and Planetary Change*, 103, 168–173.
- Mandl, G. W. (2000). The Alpine sector of the Tethyan shelf—Examples of Triassic to Jurassic sedimentation and deformation from the Northern Calcareous Alps. *Mitteilungen Österreichische Geologische Gesellschaft*, 92, 61–77.
- Márton, E., Pavelić, D., Tomljenović, B., Avanić, R., Pamić, J., & Márton, P. (2002). In the wake of a counterclockwise rotating Adriatic microplate: Neogene paleomagnetic results from Northern Croatia. *International Journal of Earth Sciences*, 91, 514–523.
- Meulenkamp, J. E., Wortel, M. J. R., Van Wamel, W. A., Spakman, W., & Hoogerduyn Strating, E. (1988). On the Hellenic subduction zone and the geodynamical evolution of Crete since the late middle Miocene. *Tectonophysics*, 146, 203–215.
- Mikes, T., Christ, D., Petri, R., Dunkl, I., Frei, D., Báldi-Beke, M., et al. (2008). Provenance of the Bosnian Flysch. *Swiss Journal of Geosciences*, 101, 31–54.
- Missoni, S., & Gawlick, H. J. (2011a). Evidence for Jurassic subduction from the Northern Calcareous Alps (Berchtesgaden; Austroalpine, Germany). *International Journal of Earth Sciences*, 100, 1605–1631.
- Missoni, S., & Gawlick, H. J. (2011b). Jurassic mountain building and Mesozoic-Cenozoic geodynamic evolution of the Northern Calcareous Alps as proven in the Berchtesgaden Alps (Germany). *Facies*, 57, 137–186.



- Mišur, I., Balen, D., Klötzli, U., Belak, M., Massonne, H. J., Brlek, M., & Brčić, V. (2023). Petrochronological study of chloritoid schist from Medvednica Mountain (Zagorje Mid-Transdanubian zone, Croatia). *Geologia Croatica*, 76(1), 13–36.
- Moro, A., Čosović, V., Benić, J., & Dokmanović, J. (2010). Taxonomy of Rudists from the Campanian Transgressive Sediments of Brašljevača, Donje Orešje and Sv. Martin, Northern Croatia. *Turkish Journal of Earth Sciences*, 19, 613–633.
- Neubauer, F., Genser, J., & Handler, R. (1999). The Eastern Alps: Result of a two-stage collision process. *Mitteilungen Gesellschaft Geologische*, 92, 117–134.
- Nirta, G., Aberhan, M., Bortolotti, V., Carras, N., Menna, F., & Fazzuoli, M. (2020). Deciphering the geodynamic evolution of the Dinaric orogen through the study of the 'overstepping' Cretaceous successions. *Geological Magazine*, 157(8), 1238–1264.
- Nirta, G., Moratti, G., Piccardi, L., Montanari, D., Carras, N., Catanzariti, R., Chiari, M., & Marcucci, M. (2018). From obduction to continental collision: New data from Central Greece. *Geological Magazine*, 155(2), 377–421.
- Palinkaš, L., Bermanec, V., Moro, A., Dogančić, D., & Strmić-Palinkaš, S. (2006). The northernmost Ni-lateritic weathering crust in the Tethyan domain, Gornje Orešje, Medvednica Mt., Mesozoic ophiolite belts of northern part of the Balkan. *Balkan Peninsula Proceedings*, 97–101.
- Pamić, J. (2002). The Sava-Vardar Zone of the Dinarides and Hellenides versus the Vardar Ocean. *Eclogae Geologicae Helveticae*, 95, 99–113.
- Pamić, J., Gušić, I., & Jelaska, V. (1998). Geodynamic evolution of the Central Dinarides. *Tectonophysics*, 297, 251–268.
- Pavelić, D. (2001). Tectonostratigraphic model for the North Croatian and North Bosnian sector of the Miocene Pannonian Basin System. *Basin Research*, 13(3), 359–376.
- Pavelić, D., & Kovačić, M. (2018). Sedimentology and stratigraphy of the Neogene rift-type North Croatian Basin (Pannonian Basin System, Croatia): A review. *Marine and Petroleum Geology*, 91, 455–469.
- Picotti, V., Romano, M. A., Ponzá, A., Guido, F. L., & Peruzza, L. (2022). The Montello thrust and the active mountain front of the eastern Southern Alps (northeast Italy). *Tectonics*, 41, e2022TC007522.
- Placer, L. (1999a). Contribution to the macro-tectonic subdivision of the border region between Southern Alps and External Dinarides. *Geologija*, 41, 223–255.
- Placer, L. (1999b). Structural meaning of the Sava folds. *Geologija*, 41, 191–221.
- Plašienka, D., Grecula, P., Putiš, M., Hovorka, D., & Kovač, M. (1997a). Evolution and structure of the Western Carpathians: an overview. In: Grecula, P., Hovorka, D., & Putiš, M. (Eds.) Geological evolution of the Western Carpathians, Mineralia Slovaca Monograph, Bratislava, pp. 1–24.
- Plašienka, D., Putiš, M., Kovač, M., Šefara, J., & Hruševský, I. (1997b). Zones of Alpidic subduction and crustal underthrusting in the Western Carpathians. In: Grecula, P., Hovorka, D., & Putiš, M. (Eds.) Geological evolution of the Western Carpathians, Mineralia Slovaca Monograph, Bratislava, pp. 35–42.
- Pleničar, M., Premru, U., & Herak, M. (1975). Osnovna geološka karta SFRJ 1:100,000, list Novo Mesto L33–79 (Basic Geological Map of SFRY 1:100,000, Novo Mesto sheet). Geološki zavod Ljubljana, Savezni geološki zavod.
- Porkolab, K., Köver, S., Benko, Z., Heja, G. H., Fiałowski, M., Soos, B., Gerzina Spajčić, N., Đerić, N., & Fodor, L. (2019). Structural and geochronological constraints from the Drina-Ivanjica thrust sheet (Western Serbia): Implications for the Cretaceous-Paleogene tectonics of the Internal Dinarides. *Swiss Journal of Geosciences*, 112, 217–234.
- Rainer, T., Sachsenhofer, R. F., Greenb, P. F., Rantitscha, G., Herlec, U., & Vrabec, M. (2016). Thermal maturity of Carboniferous to Eocene Sediments of the Alpine-Dinaric Transition Zone (Slovenia). *International Journal of Coal Geology*, 157, 19–38.
- Ratschbacher, L., Frisch, W., Linzer, H. G., & Merle, O. (1991). Lateral extrusion in the Eastern Alps, part 2: Structural analysis. *Tectonics*, 10(2), 257–271.
- Rosenberg, C. L., Berger, A., Bellahsen, N., & Bousquet, R. (2015). Relating orogen width to shortening, erosion, and exhumation during Alpine collision. *Tectonics*, 34(6), 1306–1328.
- Rožič, B., Jurkoviček, T. K., Rožič, P. Ž., & Gale, L. (2017). Sedimentary record of subsidence pulse at the Triassic/Jurassic boundary interval in the Slovenian Basin (eastern Southern Alps). *Geologica Carpathica*, 68(6), 543.
- Sarti, M., Bosellini, A., & Winterer, E. L. (1992). Basin geometry and architecture of a Tethyan Passive Margin, Southern Alps, Italy: Implications for rifting mechanisms: Chapter 13: African and Mediterranean Margins. In J. S. Watkins, F. Zhiqiang, & K. J. McMillen (Eds.), *Geology and geophysics of continental margins*. The American Association of Petroleum Geologists.
- Schefer, S. (2010). Tectono-metamorphic and magmatic evolution of the Internal Dinarides (Kopaonik area, southern Serbia) and its significance for the geodynamic evolution of the Balkan Peninsula. PhD thesis University of Basel, 230pp.
- Schmid, S. M., Bernoulli, D., Fügenschuh, B., Maženc, L., Schefer, S., Schuster, R., Tischler, M., & Ustaszewski, K. (2008). The Alpine-Carpathian-Dinaridic orogenic system: Correlation and evolution of tectonic units. *Swiss Journal of Geosciences*, 101, 139–183.
- Schmid, S. M., Fügenschuh, B., Kissling, E., & Schuster, R. (2004). Tectonic map and overall architecture of the Alpine orogen. *Eclogae Geologicae Helveticae*, 97, 93–117.
- Schmid, S. M., Fügenschuh, B., Kounov, A., Matenco, L., Nievergelt, P., Oberhänsli, R., Pleuger, J., Schefer, S., Schuster, R., Tomljenović, B., Ustaszewski, K., & Van Hinsbergen, D. J. J. (2020). Tectonic units of the Alpine collision zone between Eastern Alps and Western Turkey. *Gondwana Research*, 78, 308–374.
- Schmid, S. M., Pfiffner, O. A., Froitzheim, N., Schönborn, G., & Kissling, E. (1996). Geophysical-geological transect and tectonic evolution of the Swiss-Italian Alps. *Tectonics*, 15, 1036–1064.
- Schönborn, G. (1999). Balancing cross sections with kinematic constraints: The Dolomites (northern Italy). *Tectonics*, 18, 527–545.
- Sebe, K., Kovačić, M., Magyar, I., Krizmanić, K., Špelić, M., Sütő-Szentai, M., Kovács, A., Korecz-Szuromi, A., Bakrač, K., Hajek-Tadesse, V., Troškot-Čorbić, T., & Sztanó, O. (2020). Correlation of upper Miocene-Pliocene Lake Pannon deposits across the Drava Basin, Croatia and Hungary. *Geologia Croatica*, 73(3), 177–195.
- Šegvić, B., Slovenec, D., & Badurina, L. (2023). Major and rare earth element mineral chemistry of low-grade assemblages inform dynamics of hydrothermal ocean-floor metamorphism in the Dinaridic Neotethys. *Geological Magazine*, 160(3), 444–470.
- Šegvić, B., Slovenec, D., Schuster, R., Babajić, E., Badurina, L., & Lugović, B. (2020). Sm-Nd geochronology and petrologic investigation of sub-ophiolite metamorphic sole from the Dinarides (Krivaja-Konjuh, Ophiolite Complex, Bosnia and Herzegovina). *Geologia Croatica*, 73(2), 119–130.
- Šikić, K., Basch, O., & Šimunić, An. (1977). Osnovna geološka karta SFRJ 1:100,000, list Zagreb L33–80 (Basic Geological Map of SFRY 1:100,000, Zagreb sheet). Institut za geološka istraživanja Zagreb, Savezni geološki zavod.
- Šimunić, An. (1992). Geološki odnosi središnjeg dijela Hrvatskog Zagorja. PhD thesis, Zagreb, 208pp.
- Šimunić, An., Pikića, M., & Hećimović, I. (1982). Osnovna geološka karta SFRJ 1:100,000, list Varaždin L33–69 (Basic Geological Map of SFRY 1:100,000, Varaždin sheet). Geološki zavod Zagreb, Savezni geološki zavod.
- Šimunić, An., Pikića, M., Hećimović, I., & Šimunić, Al. (1981). Osnovna geološka karta SFRJ 1:100,000, Tumač za list Varaždin L 33–69 (Basic Geological Map of SFRY 1:100,000 Explanatory notes for Varaždin sheet). Institut za geološka istraživanja Zagreb, Savezni geološki zavod.
- Šimunić, An., & Šimunić, Al. (1997). Triassic deposits of Hrvatsko Zagorje. *Geologia Croatica*, 50(2), 243–250.
- Šimunić, An., Šimunić, Al., & Milanović, M. (1979). Geološka građa Ivanščice i Ravne gore. *Geološki Vjesnik*, 31, 157–174.
- Slovenec, D., Horvat, M., Smirčić, D., Belak, M., Badurina, L., Kukoč, D., Grgasović, T., Byerly, K., Vukovski, M., & Šegvić, B. (2023). On the evolution of Middle Triassic passive margins of the Greater Adria Plate: Inferences from the study of calc-alkaline and shoshonitic tuffs from NW Croatia. *Ofoliti*, 48(1), 31–46.
- Slovenec, D., Lugović, B., Meyer, H., & Garapić Šiftar, G. (2011). A tectonomagmatic correlation of basaltic rocks from ophiolite mélanges at the North-Eastern tip of the Sava-Vardar suture Zone, Northern Croatia, constrained by geochemistry and petrology. *Ofoliti*, 36(1), 77–100.
- Slovenec, D., & Pamić, J. (2002). Geology of the Vardar Zone ophiolites of the Medvednica Mountain area located along the Zagreb-Zemplin line (NW Croatia). *Geologica Carpathica*, 53(1), 53–59.

- Slovenec, D., & Šegvić, B. (2024). The evolution of the Mesozoic lithosphere of northwestern Neotethys: A petrogenetic and geodynamic perspective. *Journal of the Geological Society*. <https://doi.org/10.1144/jgs2023-132>
- Slovenec, D., Šegvić, B., Halamić, J., Goričan, Š., & Zanoni, G. (2020). An ensialic volcanic arc along the northwestern edge of paleotethys—Insights from the Mid-Triassic volcano-sedimentary succession of Ivanščica Mt. (northwestern Croatia). *Geological Journal*, *55*, 4324–4351.
- Smirčić, D., Aljinović, D., Barudžija, U., & Kolar-Jurkoveš, T. (2020). Middle Triassic syntectonic sedimentation and volcanic influence in the central part of the External Dinarides, Croatia (Velebit Mts.). *Geological Quarterly*, *64*(1), 220–239.
- Smirčić, D., Kolar-Jurkoveš, T., Aljinović, D., Barudžija, U., Jurkoveš, B., & Hrvatović, H. (2018). Stratigraphic definition and correlation of Middle Triassic Volcaniclastic Facies in the External Dinarides: Croatia and Bosnia and Herzegovina. *Journal of Earth Science*, *29*, 864–878.
- Smirčić, D., Vukovski, M., Slovenec, D., Kukoč, D., Šegvić, B., Horvat, M., Belak, M., Grgasović, T., & Badurina, L. (2024). Facies architecture, geochemistry and petrogenesis of Middle Triassic volcaniclastic deposits of Mt Ivanščica (NW Croatia)—Evidence of bimodal volcanism in the Alpine-Dinaridic transitional zone. *Swiss Journal of Geosciences*. <https://doi.org/10.1186/s00015-024-00453-8>
- Stach, E., MacKowsky, M. T. H., Teichmüller, M., Taylor, G. H., Chandra, D., & Teichmüller, R. (1982). *Coal petrology* (p. 535). Berlin-Stuttgart.
- Stampfli, G. M., & Borel, G. D. (2002). A plate tectonic model for the Paleozoic and Mesozoic constrained by dynamic plate boundaries and restored synthetic oceanic isochrons. *Earth and Planetary Science Letters*, *196*, 17–33.
- Stampfli, G. M., & Borel, G. (2004). The TRANSMED transects in space and time: Constraints on the paleotectonic evolution of the Mediterranean domain. In W. Cavazza, F. M. Roure, W. Spakman, G. M. Stampfli, & P. A. Ziegler (Eds.), *The TRANSMED Atlas: The Mediterranean Region from Crust to Mantle* (pp. 53–80). Springer.
- Steiner, T. M. C., Gawlick, H. J., Melcher, F., & Schlagintweit, F. (2021). Ophiolite derived material as parent rocks for Late Jurassic bauxite: Evidence for Tithonian unroofing in the Northern Calcareous Alps (Eastern Alps, Austria). *International Journal of Earth Sciences*, *110*, 1847–1862.
- Stern, G., & Wägrich, M. (2013). Provenance of Upper Cretaceous to Eocene Gosau Group around and beneath the Vienna Basin (Austria and Slovakia). *Swiss Journal of Geosciences*, *106*, 505–527.
- Tari, V. (2002). Evolution of the northern and western Dinarides: A tectono-stratigraphic approach. In G. Bertotti, K. Schumann, & S. Cloetingh (Eds.), *Neotectonics and surface processes: The Pannonian Basin and Alpine/Carpathian System, Stephan Mueller Special Publication Series* (pp. 105–120). Copernicus.
- Taylor, G. H., Teichmüller, M., Davis, A., Diessel, C. F. K., Littke, R., & Robert, P. (1998). *Organic petrology* (p. 704). Berlin-Stuttgart.
- Thöni, M. (2006). Dating eclogite-facies metamorphism in the Eastern Alps—Approaches, results, interpretations: A review. *Mineralogy and Petrology*, *88*, 123–148.
- Tomljenović, B. (2002). Strukturne značajke Medvednice i Samoborskog gorja. PhD thesis, Zagreb, 208pp.
- Tomljenović, B., & Csontos, L. (2001). Neogene-Quaternary structures in the border zone between Alps, Dinarides and Pannonian Basin (Hrvatsko zagorje and Karlovac basins, Croatia). *International Journal of Earth Sciences*, *90*, 560–578.
- Tomljenović, B., Csontos, L., Márton, E., & Márton, P. (2008). Tectonic evolution of the northwestern Internal Dinarides as constrained by structures and rotation of Medvednica Mountains, North Croatia. *Geological Society, London, Special Publications*, *298*, 145–167.
- Tremblay, A., Meshi, A., Deschamps, T., Goulet, F., & Goulet, N. (2015). The Vardar zone as a suture for the Mirdita ophiolites, Albania: Constraints from the structural analysis of the Korabi-Pelagonia zone. *Tectonics*, *34*(2), 352–375.
- Ustaszewski, K., Kounov, A., Schmid, S. M., Schaltegger, U., Krenn, E., Frank, W., & Fügenschuh, B. (2010). Evolution of the Adria-Europe plate boundary in the northern Dinarides: From continent-continent collision to back-arc extension. *Tectonics*, *29*(TC6017), 1–34.
- Ustaszewski, K., Schmid, S. M., Lugović, B., Schuster, R., Schaltegger, U., Bernoulli, D., Hottinger, L., Kounov, A., Fügenschuh, B., & Schefer, S. (2009). Late Cretaceous intra-oceanic magmatism in the internal Dinarides (northern Bosnia and Herzegovina): Implications for the collision of the Adriatic and European plates. *Lithos*, *108*, 106–125.
- van Gelder, I. E., Matenco, L., Willingshofer, E., Tomljenović, B., Andriessen, P. A. M., Ducea, M. N., Beniést, A., & Gruić, A. (2015). The tectonic evolution of a critical segment of the Dinarides-Alps connection: Kinematic and geochronological inferences from the Medvednica Mountains, NE Croatia. *Tectonics*, *34*(9), 1952–1978.
- van Hinsbergen, D. J. J., Torsvik, T. H., Schmid, S. M., Matenco, L. C., Maffione, M., Vissers, R. L. M., Gürer, D., & Spakman, W. (2020). Orogenic architecture of the Mediterranean region and kinematic reconstruction of its tectonic evolution since the Triassic. *Gondwana Research*, *81*, 79–229.
- van Unen, M., Matenco, L., Demir, V., Nader, F. H., Darnault, R., & Mandić, O. (2019a). Transfer of deformation during indentation: Inferences from the post-middle Miocene evolution of the Dinarides. *Global and Planetary Change*, *182*, 103027.
- van Unen, M., Matenco, L., Nader, F. H., Darnault, R., Mandić, O., & Demir, V. (2019b). Kinematics of foreland-vergent crustal accretion: Inferences from the Dinarides evolution. *Tectonics*, *38*(1), 49–76.
- Vermeesch, P. (2018). IsoplotR: A free and open toolbox for geochronology. *Geoscience Frontiers*, *9*, 1479–1493.
- Vishnevskaya, V. S., Djerić, N., & Zakariadze, G. S. (2009). New data on Mesozoic Radiolaria of Serbia and Bosnia, and implications for the age and evolution of oceanic volcanic rocks in the Central and Northern Balkans. *Lithos*, *108*(1–4), 72–105.
- Vrabec, M., & Fodor, L. (2006). Late Cenozoic tectonics of Slovenia: structural styles at the Northeastern corner of the Adriatic microplate. In N. Pinter, N. Greneczy, J. Weber, S. Stein, & D. Medak (Eds.), *The Adria microplate: GNSS geodesy, tectonics and hazards (NATO science series IV, Earth and environmental Sciences 61)* (pp. 151–168). Springer.
- Vukovski, M., Kukoč, D., Grgasović, D., Fuček, L., & Slovenec, D. (2023). Evolution of eastern passive margin of Adria recorded in shallow- to deepwater successions of the transition zone between the Alps and the Dinarides. *Facies*. <https://doi.org/10.1007/s10347-023-00674-7>
- Wägrich, M., & Faupl, P. (1994). Paleogeography and geodynamic evolution of the Gosau Group of the Northern Calcareous Alps (Late Cretaceous, Eastern Alps, Austria). *Palaeogeography, Palaeoclimatology, Palaeoecology*, *110*, 235–254.
- Wägrich, M., & Marschalko, R. (1995). Late Cretaceous to Early Tertiary palaeogeography of the Western Carpathians (Slovakia) and the Eastern Alps (Austria): Implications from heavy mineral data. *Geologische Rundschau*, *84*, 187–199.
- Willingshofer, E., Neubauer, F., & Cloetingh, S. (1999a). The significance of Gosau-type basins for the late cretaceous tectonic history of the Alpine-Carpathian belt. *Physics and Chemistry of the Earth, Part A*, *24*(8), 687–695.
- Willingshofer, E., van Wees, J. D., Cloetingh, S., & Neubauer, F. (1999b). Thermo-mechanical consequences of Cretaceous continent-continent collision in the eastern Alps (Austria)—Insights from two-dimensional modeling. *Tectonics*, *18*(5), 809–826.
- Winkler, A. (1923). Ueber den Bau der östlichen Südalpen. *Mitt. Geol. Ges.*, *XVI*, 1–272, Wien.
- Zattin, M., Cuman, A., Fantoni, R., Martin, S., Scotti, P., & Stefani, C. (2006). From Middle Jurassic heating to Neogene cooling: The thermochronological evolution of the southern Alps. *Tectonophysics*, *414*, 191–202.
- Zattin, M., Stefani, C., & Martin, S. (2003). Detrital fission-track analysis and petrography as keys of Alpine exhumation: The example of the Veneto foreland (Southern Alps, Italy). *Journal of Sedimentary Research*, *73*, 1051–1061.
- Zupanić, J., Babić, Lj., & Crnjaković, M. (1981). Lower Cretaceous basinal clastics (Oštrc Formation) in the Mt. Ivanščica (Northwestern Croatia). *Acta Geologica*, *11*(1), 1–44.

## Publisher's Note

Springer Nature remains neutral with regard to jurisdictional claims in published maps and institutional affiliations.